PB 189 074

A MODELING STUDY TO CHARACTERIZE PHOTOCHEMICAL ATMOSPHERIC REACTIONS TO THE LOS ANGELES BASIN AREA

A. Q. Eschenroeder, et al

General Research Corporation
Santa Barbara, California

November 1969

CLEARINGHOUSE
FOR FEDERAL SCIENTIFIC AND TECHNICAL INFORMATION

Distributed . . . 'to foster, serve and promote the nation's economic development and technological advancement.'

U.S. DEPARTMENT OF COMMERCE/National Bureau of Standards

This document has been approved for public release and sale.

PB189074

CR-1-152

A MODELING STUDY TO CHARACTERIZE PHOTOCHEMICAL ATMOSPHERIC REACTIONS TO THE LOS ANGELES BASIN AREA

FINAL REPORT
Contract No. CPA-22-69-127

November 1969

A.Q. Eschenroeder
J.R. Martinez

GENERAL RESEARCH CORPORATION
P. O. BOX 3587, SANTA BARBARA, CALIFORNIA 93105

Reproduced by the
CLEARINGHOUSE
for Federal Scientific & Technical
Information Springfield Va. 22151

74

The work upon which this publication is based was performed pursuant to Contract No. CPA 22-69-127 with the National Air Pollution Control Administration, CPE, Public Health Service, Department of Health, Education, and Welfare.

ABSTRACT

Chemical kinetics and atmospheric transport processes are combined in this finite difference formulation to compute concentration histories for photochemical smog. The kinetics are expressed as a lumped parameter reaction mechanism which was derived from laboratory data in the literature. Diffusion coefficients, which depend on height and on time, come from atmospheric measurements. Inputs consist of source inventories for the Los Angeles basin and the solar irradiation curves for the appropriate days. Predicted time histories of reactive hydrocarbons, oxides of nitrogen and ozone are consistent with the variations observed at an air monitoring station. With refined descriptions of advection, the mathematical model will serve as a tool in planning legislation and guiding urban planning in the future.

CONTENTS

SECTION		PAGE
	ABSTRACT	i
I	INTRODUCTION	1
II	A SIMPLIFIED KINETIC SCHEME	6
III	ATMOSPHERIC VALIDATION STUDIES	13
	A. Code Development	13
	B. Input Data Sources	16
	C. Validation Data Sources	21
	D. Test Results for Los Angeles Basin	22
IV	CONCLUDING REMARKS	33
APPENDIX I	FURTHER VALIDATION TESTS USING CHAMBER DATA	35
APPENDIX II	FINITE DIFFERENCE EQUATIONS FOR THE MODEL	40
APPENDIX III	SPECIFICATIONS FOR THE DATA STATISTICAL ANALYSIS PROGRAM	44
APPENDIX IV	ADDITIONAL SPECIES CONCENTRATION GRAPHS	55
APPENDIX V	EL MONTE REACTIVITY INDEX	63
	REFERENCES	65

ILLUSTRATIONS

NO.		PAGE
1	Lumped-Parameter Reaction Mechanism	7
2	Computed and Observed Reactant Histories	8
3	Computed and Observed Product Histories	8
4	Variations of Diffusivity With Height for Different Average Wind Speeds	17
5	Geographical Traffic Distribution in Los Angeles County	20
6	Los Angeles Traffic/Time Distributions	20
7	Carbon Monoxide Concentration at Huntington Park on Type 3 Day	23
8	C_2H_2/NO_x Ratios for High Oxidant Days	25
9	Hydrocarbon Reactivity at Huntington Park During the Late October 1968 Smog Episode	25
10	$(NO + NO_2)$ - Concentration Ground Level Huntington Park on Type 3 Day	27
11	High-Reactivity Hydrocarbons Concentration on the Type 3 Day	27
12	Ozone Concentration at Huntington Park on Type 3 Day	28
13	Nitric Oxide Concentration at Huntington Park on Type 2 Day 1968	30
14	High Reactivity Hydrocarbon Concentration at Huntington Park on Type 2 Days 1968	31
15	Ozone Concentration at Huntington Park on Type 2 Days 1968	32
16	Influence of Nitrogen Oxide on Trans-2-Butene Photo-Oxidation for $k_1 = 0.20\ min^{-1}$	36

ILLUSTRATIONS (Cont.)

NO.		PAGE
17	Influence of Light Intensity on Trans-2-Butene Photo-Oxidation	37
18	Computed and Observed Composition History	38
19	Three-Dimensional Calculation Grid	41
20	Sample Input Deck	49
21	Nitric Oxide Concentration on Type 3 Day	56
22	Nitrogen Dioxide Concentration on Type 3 Day	57
23	Pan Concentration on Type 3 Day	57
24	Low Reactivity Hydrocarbon Carbon Monoxide on Type 2 Days 1968 at Huntington Park	58
25	Nitrogen Dioxide Concentration on Type 2 Days in 1968 at Huntington Park	59
26	Pan Concentration on Type 2 Days in 1968 at Huntington Park	60
27	Three Dimensional Plot of High Reactivity Hydrocarbon	61
28	Three Dimensional Plot of Ozone	62
29	Hydrocarbon Reactivity at El Monte During the Late October 1968 Smog Episode	64

I. INTRODUCTION

Mathematical modeling will play a central role in our efforts to improve the quality of the urban air environment because decision-makers must anticipate the outcomes of available courses of action. Although air pollution models are still in an early stage of development, their validation will provide the link needed to establish the source emission limits required to achieve desired air quality standards. This approach can be broadened to answer questions of social and economic significance for different ameliorative strategies.

The anticipated evolution of modeling methods leads ever closer to a direct contact with out immediate problems. Whereas we are presently seeking a technical understanding of chemical interactions with transport processes, the next step is integration of this understanding in cost-benefit analyses. (In view of the difficulties arising, probably a more realistic goal is a cost-of-restoration study.) Successive improvement and confirmation of modeling techniques will offer quantitative criteria for Federal and State legislation to improve air quality by controlling mobile sources of emissions. Addressing more specific problems, local government needs criteria for urban planning to prescribe population patterns and industrial land uses that tend to preserve air quality. Hence the local application of predictive modeling influences the dispositions of both fixed and mobile emitters. At the finest level of detail a predictive model could provide the logic for the data processor in a real-time tactical system to guide decisions for temporary source shutdowns. Although we would hope that preventive policies would preclude the need for this kind of alarm system, it is possible that some communities may be moving toward unacceptable limits faster than controls can be imposed.

A mixture of empiricism with theory characterizes most of the atmospheric pollution models. Theory tells us the form of the governing equations, but experiments provide numerical values of coefficients appearing in these equations. Chemical rate and turbulent diffusion coefficients

are examples of empirical inputs. To achieve a maximum in generality, we get the needed values from experiments designed to examine elementary or unit processes. The model synthesizes these processes and its predictions are checked against observed atmospheric behavior. This closure with empirical information is called validation. Hence, we need experimental data for inputs and observational data for validation. It is clear from these considerations that success and confidence in the modeling can only be attained with the aid of measurements. Conversely, the modeler has an obligation to feed back requirements to the experimentalist. Perhaps a certain coefficient needs to be obtained more accurately or a certain class of atmospheric measurements must be added to the program to provide crucial validation data.

Much of the previous work on air pollution modeling centers on plume dispersal from fixed concentrated sources.[1,2] For these highly localized analyses the atmospheric diffusion parameters are assumed to be uniformly distributed in space, but dependent upon local wind and stability conditions. For elevated inversion bases, which frequently are a primary cause of pollution episodes, the freely diffusing Gaussian plume is sometimes joined with a uniform layer model at a downwind distance set by the ratio of vertical standard deviation to inversion base elevation.[3] Some applications of this approach superimpose exponential decays with empirical time constants to account for chemical reactions of the primary pollutants.[2] Meteorological air pollution models have been reviewed comprehensively by Wanta.[4] Three of the limitations of these methods for photochemical smog modeling are: (1) the formulation for fixed discrete sources must be reoriented to continuously distributed sources, (2) nonuniformity of vertical diffusion must be treated on a continuous basis, and (3) reactive plume solutions cannot generally be superposed because of inherent nonlinearities.

Efforts aimed at overcoming the limitations have resulted in methods ranging from modified classical treatments to entirely new formulations.

Because detailed chemical descriptions were not yet available, the paper by Frenkiel[5] on the Los Angeles basin stresses diffusive aspects of the problem by treating plume trajectories from a collection of puff sources. Other early work[6] made use of simplified chemistry in an analogue computer solution for composition histories in a network of homogeneously mixed cells. The top and bottom of each cell was assumed to be the inversion base and the ground respectively. Suggestions have been made to superimpose chemical change on a dispersion model similar to that of Frenkiel,[7] but only inert gases have been treated. Friedlander and Seinfeld[8] have formulated an approach for a reacting puff that undergoes vertical diffusion. Although only preliminary work has been reported for a binary reaction, this method will combine a photo-oxidation model with an integral method using a Lagrangian similarity hypothesis. The forms of the concentration distributions in the puff are presumably found from empirically determined probability density functions.

Presently in process is other work on photochemical smog modeling. A puff model is being developed by Dr. Lowell Wayne and coworkers at University of Southern California. Mechanistic studies of chemical kinetic schemes have been carried out by numerical integrations of the coupled rate equations for conditions appropriate to laboratory chamber experiments. Other computer investigations of this general nature include the work of Dr. Karl Westberg at the Aerospace Corporation and of Dr. Seymour Calvert at University of California--Riverside. These approaches follow the philosophy of validating the chemical scheme with laboratory data and modifying it for use in the atmosphere. Because of the rapid growth in this field, this brief review is likely to be incomplete, but it gives examples of typical methodologies.

Our mathematical modeling approach stems from a desire to incorporate the best aspects of the previous investigations in a finite difference formulation. Like other workers referred to above, we began with chemical kinetics validations using laboratory data. The schemes proposed heretofore contain anywhere from seventeen to several dozen reaction steps;

however, we have chosen a lumped parameter approach which reduces this number to seven. In contrast with previous work, our vertical diffusion grid is divided into small intervals instead of a single interval or a puff bounded by the ground and the inversion base. In practice we have used five or ten mesh stations (including the ground and inversion base). This approach is motivated by a desire to balance the degrees of refinement between the chemical and the transport aspects of the problem. To achieve the balance, some of the details appearing in separate treatments of each aspect must be simplified. Our objective is a feasible computational model of the measurable features of photochemical air pollution.

Some insights into model requirements are gained by examining length and time scales appropriate to the Los Angeles basin. The horizontal scale of the air region is tens of kilometers but the distance from ground to inversion base is usually less than 1/2 km during smog episodes. During late morning buildup of secondary pollutants, winds are only three or four kilometers per hour and the vertical diffusion coefficient averages approximately 10^{-2} km^2/hr or less. High reactivity hydrocarbons are halfway photo-oxidized about 2 or 3 hours after their appearance in the morning. If vertical diffusion approximates a random walk, the characteristic diffusion time from the ground to the inversion base can be 1 to 4 hours. A ten kilometer downwind drift also occurs within this interval. Consequently we conclude that a smog event must be modeled by treating simultaneously the processes of vertical diffusion, horizontal advection and finite rate photochemistry. Special approximations include: (1) neglecting advection for the morning hours of high traffic and light wind, (2) assuming stationary-states for certain active intermediate species, and (3) assuming homogeneous vertical mixing for afternoons when there is moderate wind and light traffic.

This paper describes the evolution and preliminary validation of our mathematical model for photochemical smog. The methodology stresses flexibility of input specifications, efficiency in computation, and conformity with observed phenomena. The two central sections of the paper

deal successively with chemical kinetic developments and validation tests. In the former, the highly complicated free radical chains triggered by photochemical primary processes are reduced to a simplified scheme. In the latter part, the realities of the atmosphere are introduced, and observational data are interpreted for some 1968 smog events in the Los Angeles Basin. To close the paper we comment on the present level of achievement and the future directions of work needed for further improvements.

II. A SIMPLIFIED KINETIC SCHEME

The photochemical reactions lead to most of the uniquely new requirements placed on this model. Before treating atmospheric studies, we must understand the action of the chemistry and describe it simply enough to keep the ultimate computer requirements within reasonable bounds. In our quest for efficiency in the model used here, we have used highly simplistic representations of chemical kinetics. There is no *a priori* assurance that the atmospheric reaction system is duplicated by the olefin-nitric oxide laboratory experiments from which we have drawn data. Furthermore, the need to augment the oxidation rate constants suggests that parallel reaction paths have been lumped together. With these reservations in mind we shall briefly examine the evolution of the reaction model.

Experimental chamber results have been computer analyzed to provide a kinetic model for the Los Angeles basin studies. In developing the model scheme we began by trying combinations of elementary reaction steps that have been suggested previously.[9-14] After many successive simplifications, we obtained the seven species by seven reaction model mechanism which is discussed here. Simultaneous solutions* of the coupled rate equations guided the evolution of the representation. We retained only those classes of rate-controlling steps needed to replicate observed concentration histories. On the other hand enough generality is included to validate the assumptions over a range of composition and light intensity conditions representative of photochemical air pollution. Hence, no claim is made that the scheme is a complete, mechanistic embodiment of the available chemical kinetic hypotheses.

Although the development and tests of the scheme are described elsewhere,[15] they will be reviewed briefly to provide continuity. Figure 1

---

*A variable step size Runge-Kutta code called PHOKIN was employed to study photo-oxidation kinetics. Typical modeling runs consumed 4 to 5 minutes of central processor time on a CDC 6400 system.

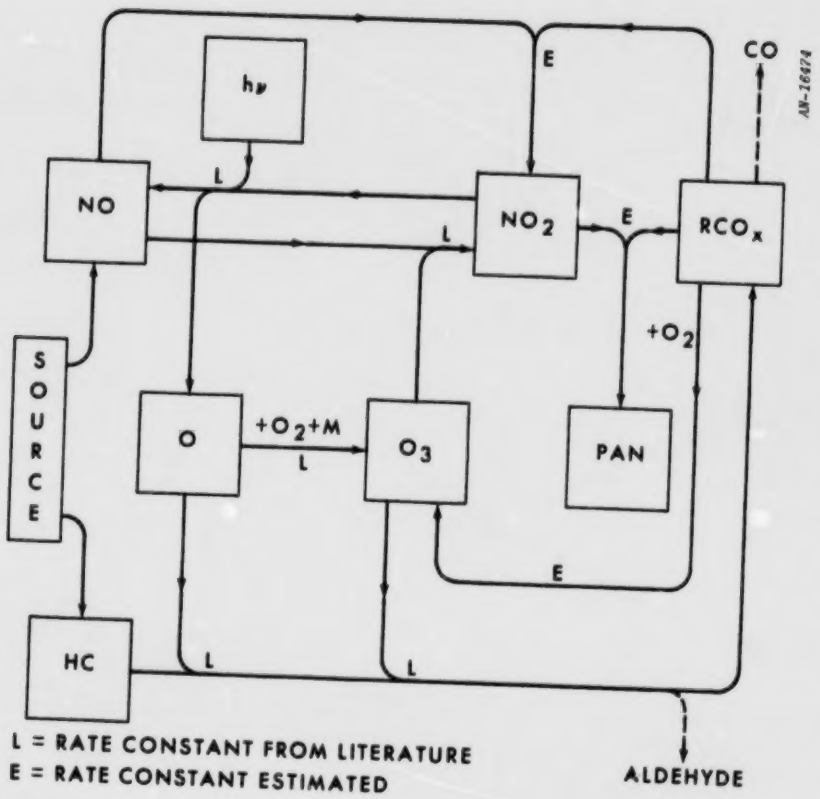

Figure 1. Lumped-Parameter Reaction Mechanism

illustrated the lumped-parameter kinetics by means of a block diagram and Figs. 2 and 3 show concentration histories in a trans-2-Butene/nitric oxide system which illustrate the action. Symbolically the diagram shows species as boxes and reactions as path intersections. In Fig. 1 the emitter is labeled "SOURCE" and sunlight is denoted by "$h\nu$" . The experiment[16] illustrated in Figs. 2 and 3 replaces the source with a premixed charge of HC and NO and employs simulated sunlight.

Examination of Fig. 1 shows that the NO_2 photodissociates to contribute O-atoms and NO . The O-atoms attack the hydrocarbon and produce free radicals represented here by RCO_x . In turn, the RCO_x provide an oxygen source for reconversion of NO to NO_2 . This path augments the already rapid reaction of ozone with NO to form NO_2 . Three-body association of O with O_2 contributes most of the ozone; however, an abstraction reaction of O_2 with RCO_x also provides ozone. Nitrate formation removes NO_2 in chain termination reactions. One minor branch of the chain is included in Fig. 1 as the production of peroxyacetyl nitrate (PAN). This is included in the model because PAN has been established to be a phytotoxicant.

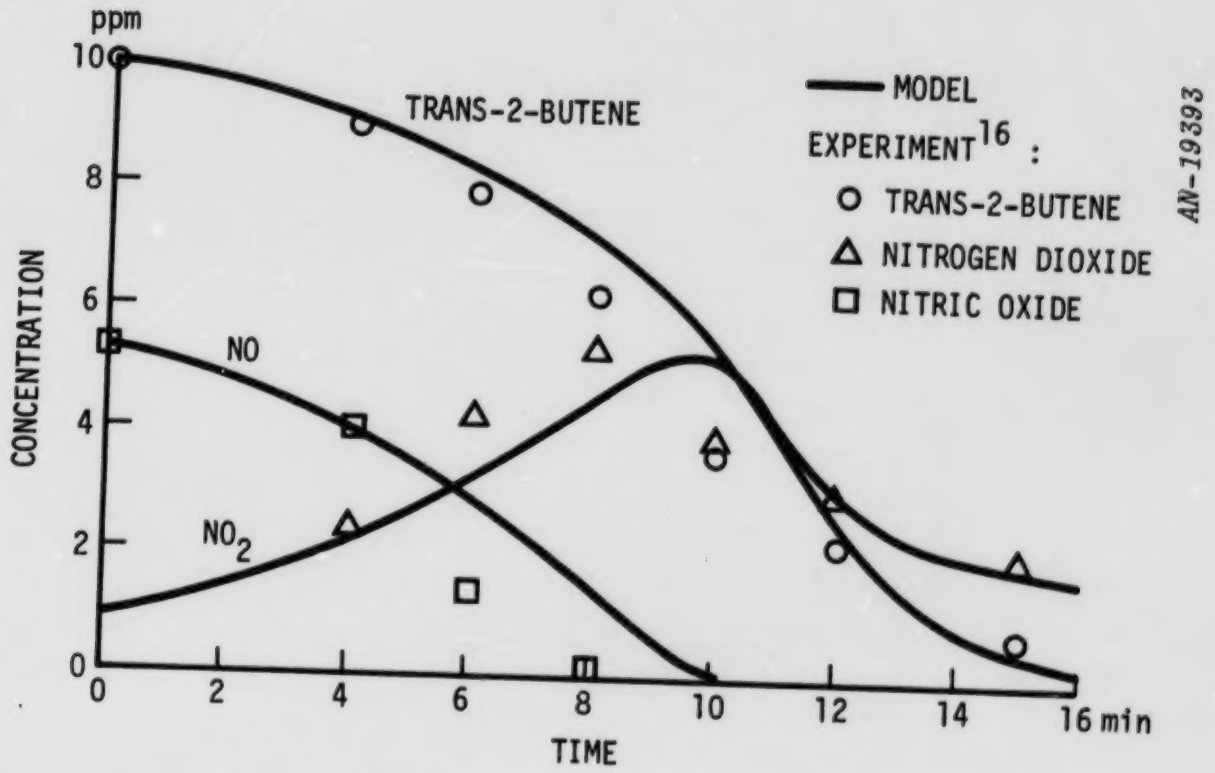

Figure 2. Computed and Observed Reactant Histories (Rate Coefficients in Table 2)

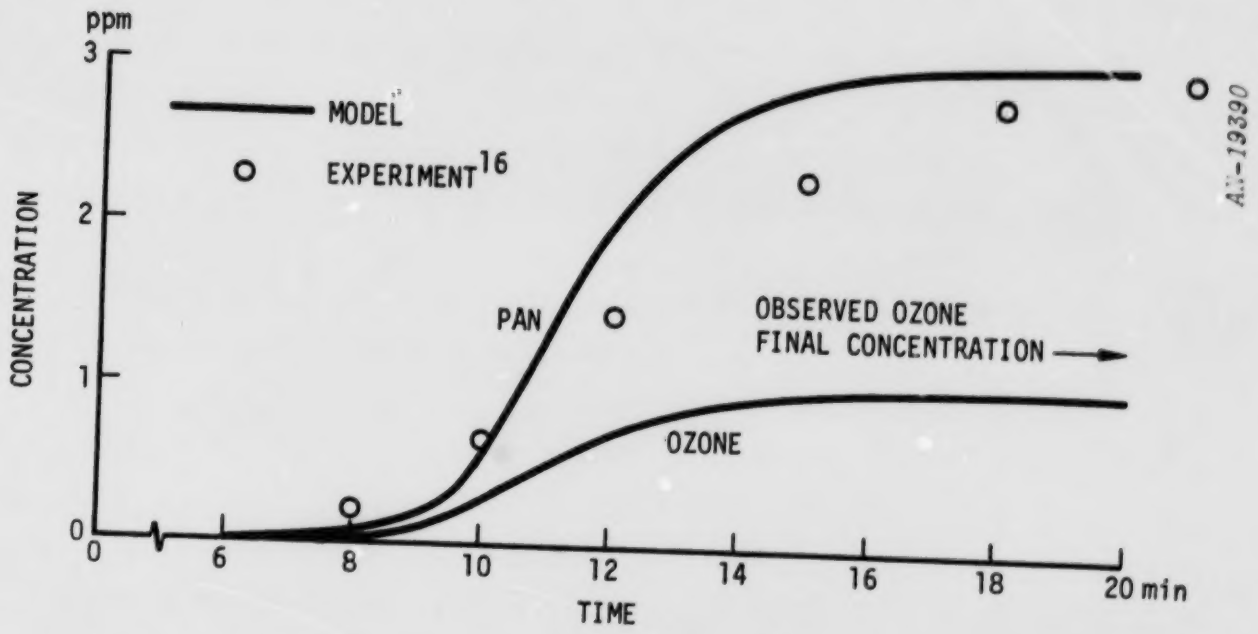

Figure 3. Computed and Observed Product Histories (Same Conditions as Those for Figure 2)

Following the concentration histories in Figs. 2 and 3, we note that the hydrocarbon disappearance contributes RCO_x which oxidizes NO up to NO_2. When this induction phase is complete, ozone concentration rises because there is no longer any NO to compete for the ozone. Nitrate formation and photodissociation then take over to reverse the rising trend in NO_2. In the later stages, ozone becomes a serious competitor with oxygen atoms in the attack on hydrocarbons.

Before we assess the validity of the calculations, we shall enumerate some of the processes which are absorbed in certain overall steps so that the simplicity of the scheme is preserved for ultimate economy in computation. First, free radicals like RCO_x or OH also attack hydrocarbons so that the O + HC and O_3 + HC rates must be artifically elevated. Second, aldehyde photolysis[17] is an additional branch of the mechanism that must be absorbed in the rates and stoichiometry of a lumped parameter scheme. Third, inorganic particulate nitrate products would be added if it were necessary to complete the material balance to account for nitrogen.[18] Fourth, radical regeneration involving CO may be implicitly absorbed in the chain branching factor applied to RCO_x.[19]

Curves in Figs. 2 and 3 illustrate calculated results* for the conditions of one of Tuesday's experiments. Table 1 details the reaction stoichiometry and rate constants for the calculation. The calculated photo-oxidation rates for the main reactants are somewhat slow around 8 minutes time and the appearance rate of PAN is too fast between 12 and 16 minutes time. This results from a compromise needed because of a certain inflexibility in the schematic kinetics. The calculation employs established values of rates from the literature for the three inorganic reactions. The NO_2 photolysis was calibrated[16] according to the light intensity at $0.37\ min^{-1}$ and the other two reaction rate constants were obtained

*Quasi-stationarity is assumed for O-atom and RCO_x-radicals to facilitate calculations. Numerical tests confirm the validity of these approximations.

TABLE 1

RATE COEFFICIENTS FOR TRANS-2-BUTENE/NITRIC OXIDE SYSTEM

Reaction	Nominal Values*	Validation Values**
$h\nu + NO_2 \rightarrow NO + O$	0.072 to 0.55 min^{-1}	0.072 to 0.55 min^{-1}
$O + O_2 + M \rightarrow O_3 + M$	1.32×10^{-5} $ppm^{-2}min^{-1}$	1.32×10^{-5} $ppm^{-2}min^{-1}$
$O_3 + NO \rightarrow NO_2 + O_2$	21.8 $ppm^{-1}min^{-1}$	21.8 $ppm^{-1}min^{-1}$
$O + C_4H_8 \rightarrow 2.5\ RCO_x + 0.12$ Ald.	3.34×10^{4} $ppm^{-1}min^{-1}$	1.11×10^{5} $ppm^{-1}min^{-1}$
$O_3 + C_4H_8 \rightarrow 2.5\ RCO_x + 0.12$ Ald.	4.2×10^{-2} to 6.4×10^{-1} $ppm^{-1}min^{-1}$	6×10^{-1} $ppm^{-1}min^{-1}$
$RCO_x + NO \rightarrow NO_2$	$\leq$ 50 $ppm^{-1}min^{-1}$	50 $ppm^{-1}min^{-1}$
$RCO_x + O_2 \rightarrow 0.5O_3$	$\leq$ 50 $ppm^{-1}min^{-1}$	5×10^{-6} $ppm^{-1}min^{-1}$
$RCO_x + NO_2 \rightarrow 0.67$ PAN	$\leq$ 50 $ppm^{-1}min^{-1}$	6 $ppm^{-1}min^{-1}$

*See Sec. II for sources.

**Values consistent with experimental measurement.[16]

from Ref. 20, assuming an ambient temperature of 27°C. The O-atom on C_4H_8 rate was increased nearly fourfold to absorb the competing radical reactions and the ozone on C_4H_8 rate fell near the upper end of measured range. Nominal values for these reactions are obtained from the literature.[12] Collision theory estimates yield upper limit nominal values for the last three reactions listed in Table 1.

All of the discussion has centered on a single experiment to illustrate the validation of the simple scheme. Other experiments bring out special features. For example, the ozone reaction with a hydrocarbon is actually far more complex than a single step because somewhat lower rate values for $O_3 + C_4H_8$ (still in the nominal range shown in Table 1) are observed in experiments involving C_4H_8/NO_2 systems under irradiation. Apart from this complication, the set of rates in Table 1 exhibit good modeling results over the various values of C_4H_8/NO-ratio and light intensities appropriate to the atmospheric problem.* Several features of this particular system, however, are atypical of photochemical air pollution. Such features include the reactivity, the concentration levels, the time scales and the organic nitrate production. Trans-2-Butene is far more reactive than the average of atmospheric hydrocarbons. Even omitting low reactivity components (methane, ethane, and acetylene) from automotive exhaust compositions we find that the remaining fraction of hydrocarbons has a weighted average reactivity index[21] many times less than that of the butenes. Regarding concentration levels, the experiment[16] cited begins with 10 ppm reactive hydrocarbon whereas atmospheric values are ten times less. As a result of these two differences smog reaction times are close to 20 times longer than those of the experiment. Finally the PAN yields from butene oxidation exceed those of the atmospheric reactants. Despite these limitations, Ref. 16 covers a broader scope of parametric variables than most experiments reported in the literature.

---

*Appendix I summarizes further validation results for C_4H_8/NO and C_3H_6/NO systems.

Therefore, it gives many validation benchmarks for various compositions and light intensities. Since the propylene-nitric oxide system is more nearly like reactive systems in air pollution, validation tests were conducted on that system also.* Again, measured composition behavior from chamber irradiation tests[22,23] serves as a basis for modifying some of the rate constants to absorb the additional effects. Lower oxidation rates and lower PAN yields occur with propylene compared with trans-2-butene. Lumped rate constants for $O + C_3H_6$ and $O_3 + C_3H_6$ were found to be 4.97×10^4 and 1.8×10^{-1} ppm^{-1} min^{-1} respectively. These were used as baseline rate constants for initiating validation studies in the Los Angeles atmosphere.

*Appendix I gives an example of the propylene studies.

III. ATMOSPHERIC VALIDATION STUDIES

A. CODE DEVELOPMENT

Having a simplified chemical scheme, we now turn our attention to incorporating it in an atmospheric transport model. We have sought approximations appropriate to air basins subject to photochemical pollution. Because of the severity of the problem and the availability of data, the Los Angeles basin area serves as the object of validation studies.

Probably the most characteristic causative factor in Los Angeles smog is the lid created by the stagnation of warm air subsiding on the cool marine layer. Late in the summer, air flows from an anticyclone over the Pacific Ocean and compresses as it loses altitude in its outward course. Onshore movement of marine air under this outflow maintains a buoyantly stable interface at the base of the elevated inversion which is marked by a temperature increase with height. Sometimes this inversion base starts out at ground level in the morning. This condition, which is chronic and of large scale, should not be confused with the transient inversions due to nocturnal radiative cooling.

The regularity exhibited by this phenomenon holds the key to extensive reduction in atmospheric model detail. As mentioned in the introduction, the relatively thin (marine) layer between the ground and the inversion base contains the bulk of the pollutants. The diurnal horizontal flow patterns within the marine layer are almost reproducible from day to day of the smog season. Only slight variations in height (above land) are experienced by the elevated inversion base over any given day. Some of the best detailed data illustrating these points are found in a report by Neiburger and Edinger.[24] A subsequent report[25] in the same series has some graphs which associate smog events with the meteorological conditions.

The entire picture described above strongly suggests that we make a marine layer model with a prescribed internal flow field. The top of the layer is nearly as wall-like as the bottom because vertical disturbances are strongly resisted by buoyant forces. Therefore, very little Reynolds stress momentum transfer occurs across the interface just as there is almost no normal transport of species (a property with which Angelenos are very familiar).

For the species budget along a streamtube in the marine layer, we assume a channel like flow with zero flux through the top "wall" and some specified flux from the ground. In choosing boundary conditions for the balance equations governing free radicals we are confronted with the usual uncertainties regarding wall catalycity. Computational tests ranging from infinite to zero catalytic efficiency for removal of oxygen atoms and RCO_x result in unimportant differences at instrument elevations of several meters because the radicals achieve local stationarity much faster than they diffuse over several meters.

The governing species equation is taken to be

$$\frac{\partial c_j}{\partial t} + u \frac{\partial c_j}{\partial x} = \frac{\partial}{\partial z} \left(D \frac{\partial c_j}{\partial z} \right) + R_j \quad (j = 1, 2, 3, \ldots, s) \quad (1)$$

where

c_j = mass concentration of jth species

t = time

u = advective downwind velocity

x = downwind distance

z = height

D = vertical turbulent diffusion coefficient

R_j = production rate for jth species

s = number of species.

Mean vertical advection is suppressed by the channel-like character of the marine layer and horizontal diffusion is relatively unimportant because of a nearly uniform distribution of emission sources. Hence these terms do not appear in Eq. 1. The chemical source term is calculated from the usual rate expressions.

Since a significant period following sunrise on a high smog day has little wind, much is to be learned by omitting the second term and studying slab solutions of the heat-equation-with-sources form. When significant winds occur, they are predominantly onshore from the west over much of the central Los Angeles basin. (A complete network implementation will include the $v(\partial c_j/\partial y)$ term in addition.)

The numerical solution of Eq. 1 follows a Crank-Nicholson type implicit finite difference scheme.[26] Since fields for u and D are prescribed by meteorology inputs, the nonlinearity is confined to some members of the R_j-terms . Because the coupling of the species equations is less severe than it is with reacting boundary layers, the general matrix inversion approach[27] is bypassed in favor of a quasi-linearization technique[28] requiring inversion of tridiagonal matrices only. Midinterval estimates (in time steps) are obtained by Taylor expansion in the leading iteration and by taking arithmetic mean values in successive iterations. Adequate convergence is obtained after three or four iterations and time steps are variable in size adapting to chemical changes. For cases including the advection term, cross iterations are employed.*

DIFKIN is a code version which solves diffusion coupled with kinetics in the absence of horizontal advection. TADKIN is the name for a Time-dependent Advection-Diffusion-Kinetics code. The first checks of DIFKIN were made for classified solutions of the heat equation. Solutions of

---

*Appendix II describes the difference equations and their solution in greater detail is given here.

400 time steps showed minimal artifical diffusion (maximum concentration error of 2% on the worst part of the profile). Sudden application of constant flux and sudden change of wall value were each tested. Binary chemistry with a single reaction step was then introduced and runs were hand checked.

Tests beyond those described have been made for carbon monoxide data from the Los Angeles basin to check estimates for source emission fluxes as well as those for diffusion coefficients. Before these results are presented, some consideration will be given to the sources of data employed for both inputs and validation tests.

B. INPUT DATA SOURCES

Except for initial profiles, the input data for the model are the meteorological conditions and the source emission conditions. Wind speed and diffusion coefficients depend on both position and time. Source inventories include the flux of each primary pollutant as it depends upon location in the basin and time of day.

Empirical parameters governing atmospheric dispersal pervade the literature on this subject. Like most cases of turbulent transport, elimination of a disposable coefficient in one place leads to a reappearance of one somewhere else. The present work uses an experimentally determined turbulent diffusion coefficient, D, in Eq. 1. Near the ground and near the inversion base we must assign a height (z) dependence to the diffusion coefficient.

Going up from the ground the functional dependence assumed for D upon z allows a linear increase to some constant value. At intermediate levels D is held constant, but approaching the inversion base a linear decrease with height is assumed. A variation on the lower part of the profile has been to maintain the ground value up to some point prior to initiating the linear increase. This variation causes little change from

the original trapezoidal profile. The elevation where constancy is achieved varies from 40 to 100 meters depending upon meteorological conditions.

Figure 4 shows typical values of the turbulent diffusion coefficient we assumed for our model compared with the values either derived or observed by other investigators. At a wind speed of 1 m/s a surface value of 30 m^2/min is high compared with Pasquill's[29] values at 200 centimeters elevation, but we use it because effective roughnesses in an urban area far exceed those of "mud flats" or "high grass". The assigned plateau value is slightly higher than that for the residual turbulence of free air attributed to Rossby and Montgomery[30] in Priestley's monograph.[31] The decrease approaching the inversion base is introduced to reflect the wall-like inhibition of vertical turbulent motion by buoyant stability.

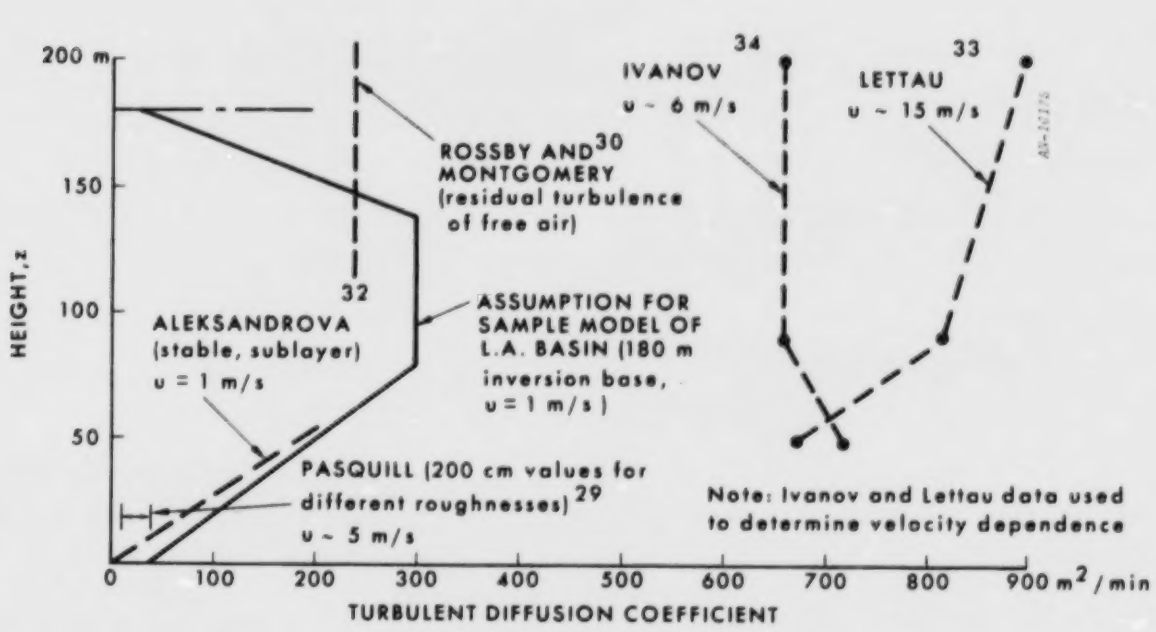

Figure 4. Variations of Diffusivity with Height for Different Average Wind Speeds

Note on Fig. 4 that the sublayer region corresponds closely to the values deduced from Aleksandrova's formulas and mast measurements for the precipitation of a puff released from a point source.[32] The values reported by Lettau[33] (as "Austauch" coefficients) were obtained from Leipzig wind profile measurements. The data of Ivanov[34] for mean square velocity and dissipation rate were used in Hanna's[35] empirical formula to obtain the 6 m/s values. Neither the Ivanov nor the Lettau results were obtained for stable lapse conditions. The assumed values for the coefficient correspond closely to the turbulent transport observed by Craig,[36] who measured water vapor profiles 30 miles offshore as warm air moved seaward across Massachusetts Bay. For light winds, values of 6 to 12 m^2/min were observed at elevations of 1 to 2 meters. At 60 to 80 meters elevation, diffusion coefficients up to 300 m^2/min were found with 6-m/s wind speeds with reduced stability. The plateau value in our profile, therefore, may be expected to vary with wind speed approximately like $50(u+5)$ m^2/min where u is in m/s . This simple relationship has been employed based on the cited findings.

Wind speed, wind direction, and inversion base height are the principal meteorological inputs. Wind data are obtained from Scott Research Laboratories (SRL) measurements[39] and from other observation stations in the area.[40] Inversion data are deduced from airborne temperature measurements[39] where possible and from morning soundings reported by the LAAPCD.[41]

Even more difficult than the turbulent diffusion estimate are those for surface emission fluxes of hydrocarbon, nitric oxide and carbon monoxide species. Originally we did a simple statistical estimate on moving sources based on the California Driving Cycle for a velocity distribution function and a packing density based on a car length spacing for every ten miles per hour speed for all the arterials and freeways in the basin. Although we arrived at surprisingly realistic values for tonnages of emission and total cars on the road, we switched to the more accurate Los Angeles County Air Pollution Control District (LAAPCD) inventory estimates[37]

based on gasoline consumption when they became available. Table 2 summarizes some of the totals from this official publication. Since tons per day are given one can compute average surface fluxes knowing that the basin comprises some 1250 square miles according to the same publication.

Additional adjustments must be made for the fact that the source emission strengths are not uniformly distributed in either time or space. To approximate the automotive sources we used the data reported by Teague[38] for the geographical (see Fig. 5) and the temporal (see Fig. 6) distributions. For nonautomotive sources averages were employed as constant background emissions. The tonnage partitioning between high reactivity and low reactivity hydrocarbons from automotive sources roughly represents the ratio of compounds having nonzero reactivity index to those having a zero value in automotive emissions. The reactivity index used here refers to a scale suggested by Caplan[21] which places methane, ethane, propane, benzene, acetylene, and methylacetylene on the zero end of the range. It should be pointed out while this scale is not a direct measure of NO to NO_2 conversion, it gives a means of partitioning the hydrocarbons into two subgroups.

TABLE 2

CONTAMINANTS IN TONS PER DAY

FROM MAJOR SOURCES WITHIN LOS ANGELES COUNTY[37]

Major Source	Organic Gases			Particulates	NO_x	SO_2	CO	Total
	Reactivity							
	High	Low	Total					
Motor Vehicle	1255	475	1730	45	645	30	9470	11,920
Non-Motor Vehicle	200	620	820	55	305	195	225	1,610
Total	1455	1095	2550	110	950	225	9695	13,530

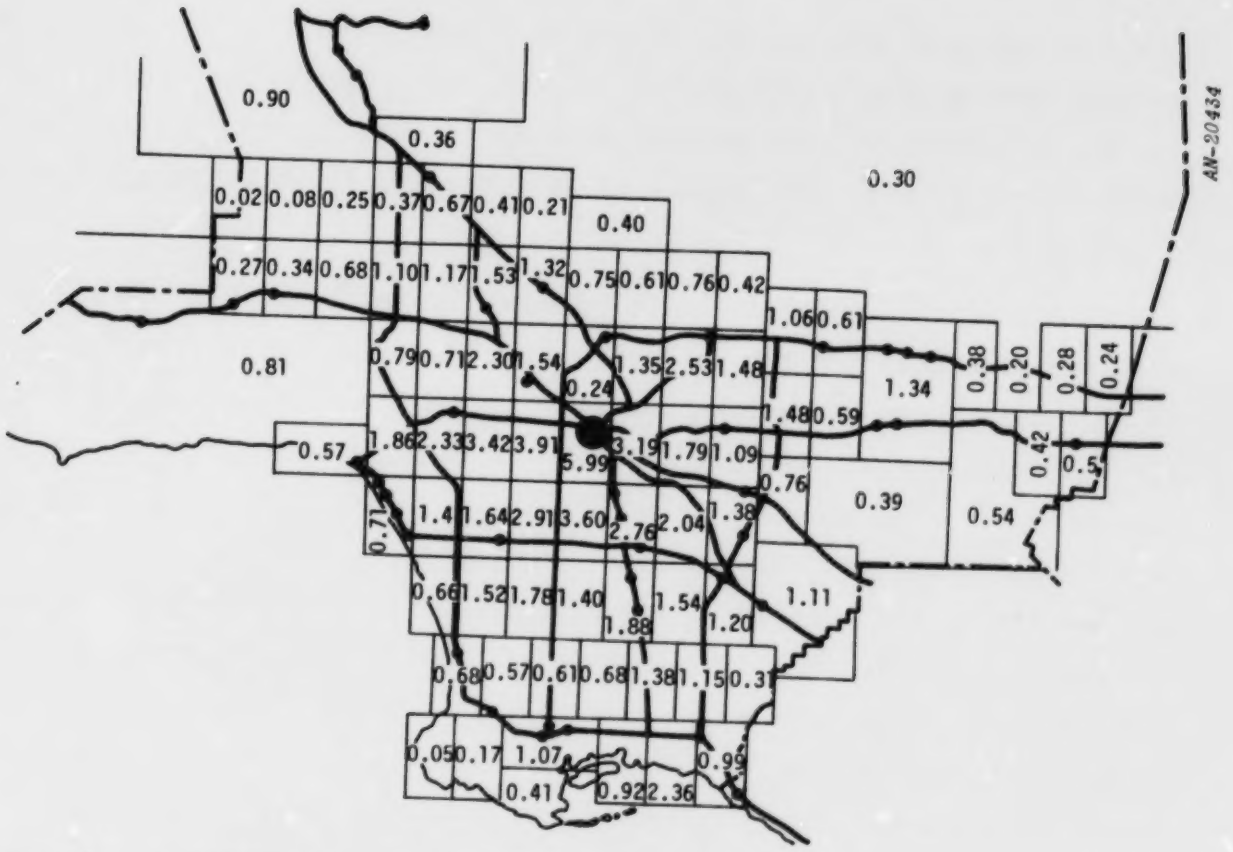

Figure 5. Geographical Traffic Distribution in Los Angeles County. Numbers shown represent percentage of County's daily traffic, in car miles, occurring in area (Ref. 38)

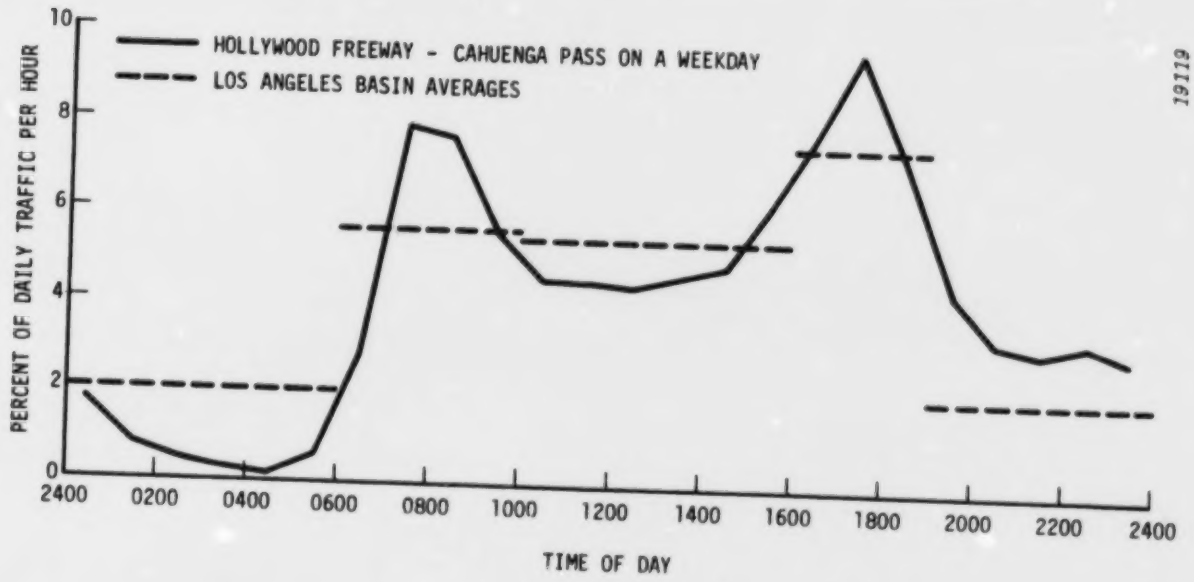

Figure 6. Los Angeles Traffic/Time Distributions

C. VALIDATION DATA SOURCES

With the atmospheric and emission source inputs, we test the model by predicting time histories of the concentration field in the marine layer. The predictions are then evaluated against a background of validation data. The primary source of these data is the SRL report[39] for the 1968 smog season (Aug. 22 to Nov. 14, 1968).

Because Volume I of Ref. 39 contains detailed descriptions of the measurements program, it will be reviewed here only briefly. Two fixed sites, Huntington Park and El Monte, California had instrumented trailers which monitored pollutant concentrations, meteorological data and ultraviolet radiation. The sites are 12.7 miles apart and lie along a prevailing air trajectory. The great step forward in this program was the resolution of hydrocarbon concentrations into more than 100 individual species up to C_{10} with a sensitivity to levels below one part per billion using highly refined gas chromatography techniques.

Limited use of other data has been made to supplement the SRL measurements. In 1967 a joint study was made by the National Center for Air Pollution Control, the California Air Resources Board Laboratory, and the Los Angeles Coun y Air Pollution Control District. The objective of the study was directed toward improvement in detailed chemical measurement. It involved air sampling at two sites, Downtown Los Angeles and Azusa. Some of the reduced data[42] have been used in the validation studies. The LAAPCD monitors concentrations over nine station network. We have used some of this information from 1968 to augment the SRL data.

The large volume of field data must be assimilated by some form of preprocessing* before it is useful for validation tests. Two states of reduction which we have employed are sorting days by type characterized

---

*Appendix III gives specifications and formats for the data statistical analysis program.

by peak oxidant* and then averaging data over all days of each given type. Consistent with the lumped parameter approach, we reduce the hydrocarbon ensemble by grouping compounds into brackets on a reactivity scale. For a beginning only two reactivity classes have been employed in accordance with the source inventories shown in Table 2. Low reactivity hydrocarbons include methane, ethane, propane, acetylene, methylacetylene and benzene. All others are considered to be high reactivity.

D. TEST RESULTS FOR LOS ANGELES BASIN

In order to concentrate on diffusion effects, and in addition to studying the chemistry using chamber data, we studied atmospheric transport of inert and low reactivity species. For initial validation tests, Huntington Park is superior to El Monte because of the symmetry in surrounding source distribution, the remoteness from any mountain interferences, and the regularity in the data. Our search for type 3 days turned up Oct. 23, 1968 as the only one with sufficient data for validation. This was used for the initial DIFKIN tests because the low wind speeds minimize the error in omitting the horizontal advection term.

Figure 7 shows results for ground level carbon monoxide concentrations at Huntington Park. This species is practically inert so that the results are a test of the transport formulation and the chemical source term for carbon monoxide is neglected. Using measured values to start at 0600,** we computed the solid curve from DIFKIN (no advection) and the dashed curve from TADKIN (input wind observations). Comparison of SRL

---

* Days are typed by peak oxidant as follows: type 0, both stations < 20 pphm ; type 1, either station 20-30 pphm ; type 2, either station > 30 pphm ; type 3, either station > 30 pphm and western station peak ≥ eastern station peak. Western and eastern stations are taken to be Huntington Park and El Monte for SRL data, or Downtown Los Angeles and Azusa for LAAPCD data.

** Using airborne sample measurements with ground measurements for type 2 days, we determined the early morning profiles to be well approximated by an exponential decrease with height using a 150-meter scale height.

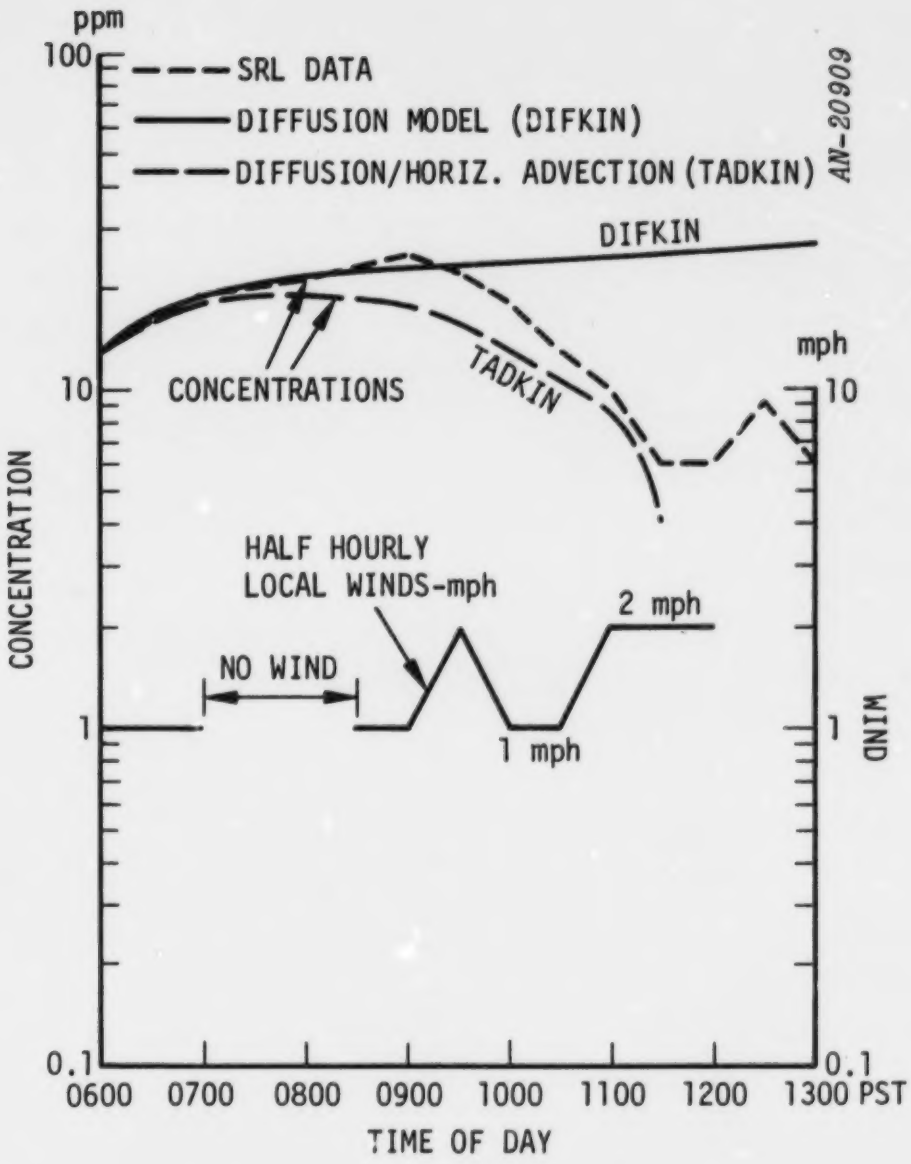

Figure 7. Carbon Monoxide Concentration at Huntington Park on Type 3 Day

data with output from the models shows that advection only becomes significant after the first three hours. Good agreement is exhibited by the models (using input data described above) with the validation data. The ventilation behavior is consistent with the local wind speeds displayed on an auxiliary graph on Fig. 7.*

Test results with photochemistry have been obtained for type 2 and 3 days using the DIFKIN code. Prior to discussing these results it is necessary to digress briefly and examine some special features of the data. First, consider the ratio of acetylene (C_2H_2) to total oxides of nitrogen (NO_x). In morning samples C_2H_2 is essentially unreacted and the NO_x has not been depleted much by the chain breaking reactions. Hence we should expect a plateau of the C_2H_2/NO_x ratio characteristic of motor vehicle exhaust. Previous investigators[42] have shown this ratio to be about four times that typifying automobile exhaust from the California Driving Cycle.** These results are displayed on Fig. 8 suggesting that the estimates from Table 2 may need modification. If we assume that nitric oxide, the emitted pollutant, is depleted in preference to C_2H_2 (say by heterogeneous reactions) then we should lower the NO_x estimates. This hypothesis is tested below.

Another consideration in the chemistry is the rate constants to employ for the O + HC and O_3 + HC reactions. The high reactivity fraction of exhaust hydrocarbons may behave initially as propylene, but selective depletion of high reactivity compounds soon slows the overall oxidation rate. Thus, the collective rate constant must shift from something near propylene to some lower value. Indeed Fig. 9, which is a plot of reactivity index versus time, shows values ranging from 1/2 to 1/3

---

*Among the auxiliary graphs in Appendix IV are plots of low reactivity hydrocarbons compared with CO for both type 2 and type 3 days.

**This is observed for high oxidant days in 1967.

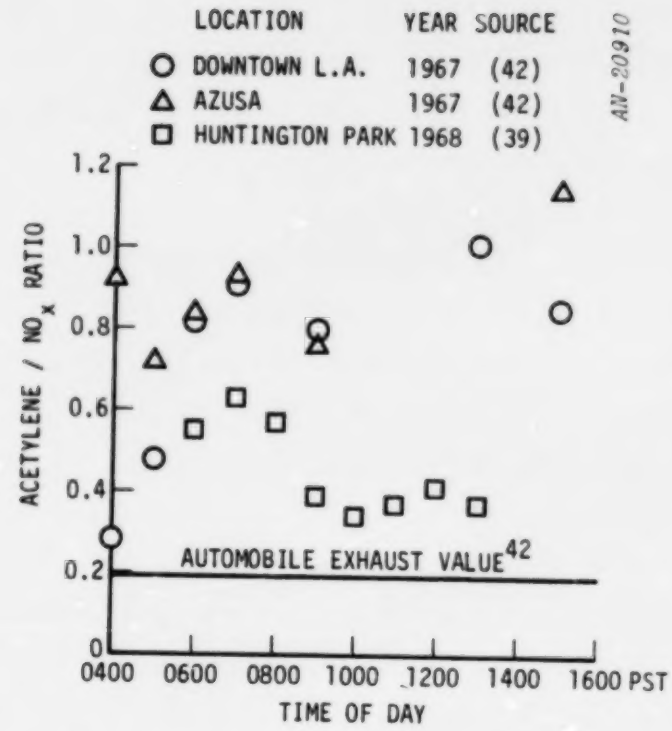

Figure 8. C_2H_2/NO_x Ratios for High Oxidant Days

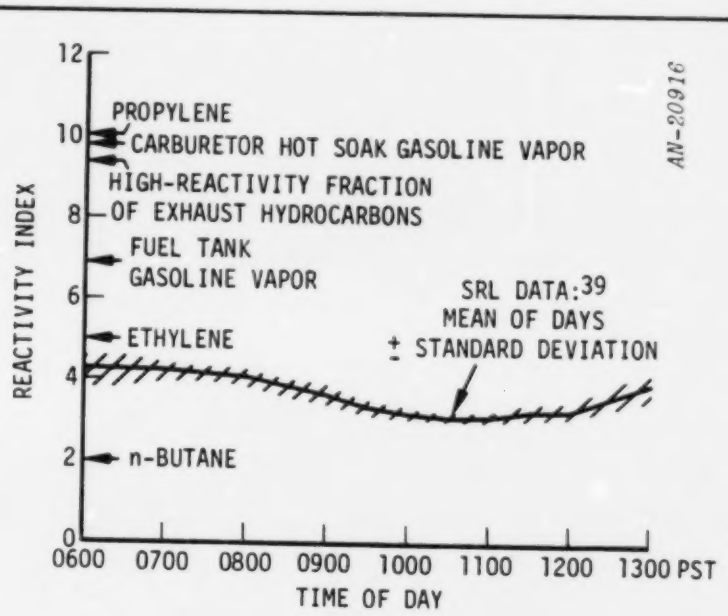

ASSUMPTIONS IN CALCULATIONS:

1. MOLE WEIGHTED AVERAGES
2. REACTIVITY SCALE DUE TO CAPLAN[21]
3. INCLUSION OF ONLY THOSE COMPOUNDS OF NON-ZERO SPECIFIC REACTIVITY

Figure 9. Hydrocarbon Reactivity at Huntington Park During the Late October 1968 Smog Episode

that of high reactivity exhaust hydrocarbons.* Although this reactivity scale may not be a direct measure of reaction kinetic parameters, it is used here for purposes of comparison.

The initial tests of the model (DIFKIN) combining diffusion with kinetics were conducted for the type 3 day. Both the rate ratio and NO_x flux ratio hypotheses were tested as shown on Figs. 10, 11, and 12. The first set of graphs illustrates most clearly the need for a downward adjustment in the nitric oxide flux if acetylene is conserved. Consistent with the results of Ref. 42, Fig. 8 suggests a factor of 4 (or more) reduction. Using $f = 1/4$, (a fourfold flux reduction) we see a great improvement in the model predictions in the NO_x curves on Fig. 10. The ratio of rates is examined in these three figures by comparing curves B, C, and D. Evidently something between 1/2 and 1/3 the propylene oxidation rate constants gives the best agreement with the observed values.[39] This tends to support the hypothesis that the reactivity index goes like the oxidation rate constants in the results shown in Fig. 9.**

The fourfold NO_x flux adjustment raises serious questions regarding either the model, the input data, or the physical processes occurring. One wonders whether some uncertainties in the reaction kinetic or turbulent diffusion parameters could account for this large a disparity instead of the alteration in the NO_x-flux . Regarding the reaction kinetics, we observe on Fig. 10 that even at the low fluxes (curves B, C, and D) the NO_x curve is controlled by diffusion rather than reactions until 0830 PST when the curves branch out. The fact that diffusion dominates is also illustrated by the large slope difference in Fig. 10 at 0600 PST. Looking back at Fig. 7 we note that the carbon monoxide buildup is modeled well by both DIFKIN and TADKIN calculations until 1000 PST. This is

---

* Appendix V contains a discussion of reactivity data at El Monte.

** Appendix IV supplies additional curves illustrating validation for type 3 days.

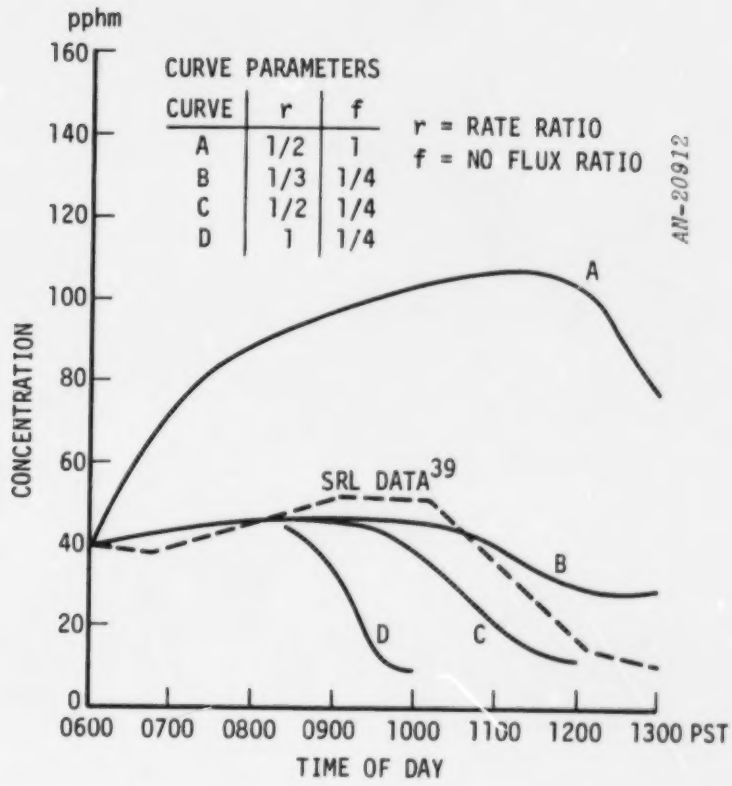

Figure 10. $(NO + NO_2)$ - Concentration Ground Level Huntington Park on Type 3 Day

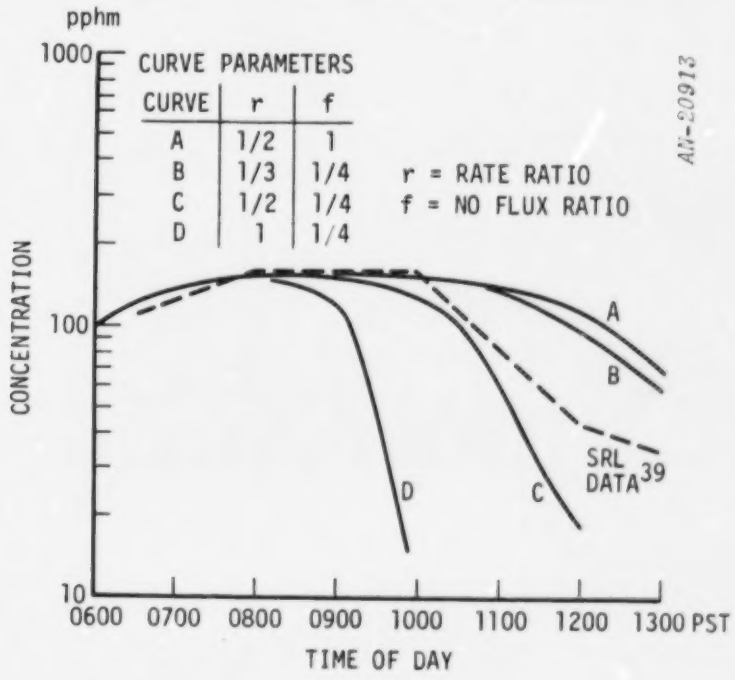

Figure 11. High-Reactivity Hydrocarbons Concentration on the Type 3 Day

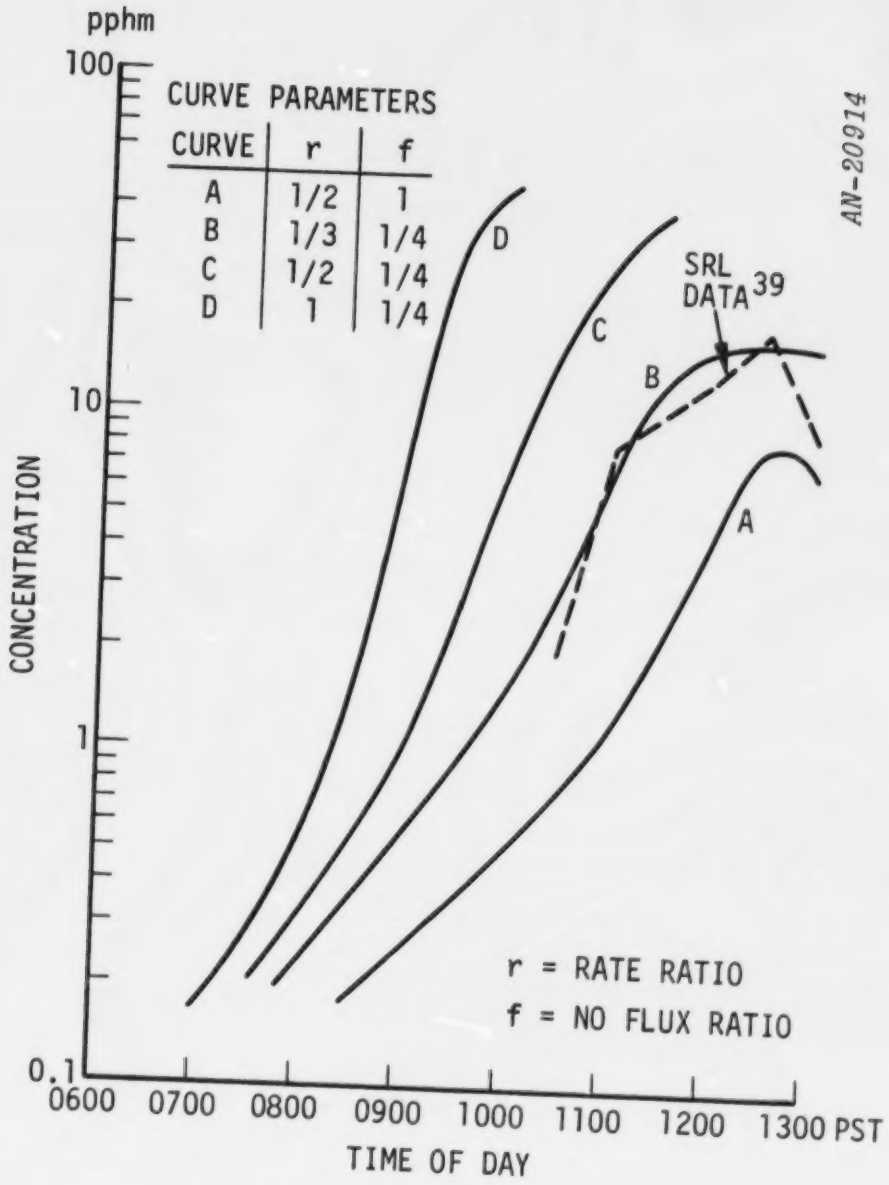

Figure 12. Ozone Concentration at Huntington Park on Type 3 Day

based on source inventory data from the same reference as that used for the NO_x curves. Thus, atmospheric diffusion uncertainties are difficult to invoke as being significant in explaining the NO_x-disparity . Oxidation rates between those in curves B and C include nearly all of the observations plotted in Figs. 10, 11, 12, 21 and 22. Similar observations will be made regarding type 2 days. Thus, it appears that the uncertainties in parameters other than the NO-flux are not sufficient to explain the apparent factor of four variation. Because of the limited sample of observations, this surprising result cannot be fully confirmed at this time. Further work and more detailed studies must be devoted to the NO_x anomaly.

Expanding the validation data to a larger sample, we selected type 2 days for which data were available during the 1968 smog season. The statistical preprocessing program derived half-hourly means and standard deviations for this sample of days. Hatched areas on Figs. 13, 14, and 15 show the mean values plus or minus one standard deviation. Again, the DIFKIN modeling was tested using five mesh stations including the ground and the inversion base. Moreover, a homogeneous mixing model was demonstrated. This model assumes that anything entering the marine layer from the ground is vertically mixed instantaneously. Reactions proceed according to the kinetic model derived in Sec. II. For all of the results in Figs. 13-15, the curve parameters are $f = 1/4$ and $r = 1/2$. Average profile values at 0600 PST and at 0900 PST are used to initiate homogeneous mixing runs. Some of the precision of detail is lost in this approximation. Considering homogeneous mixing calculations only require 5 to 10 percent of the central processor time needed by the five-station diffusion runs, they may well be useful for cases where parametric effects are studied for many different conditions.*

*Appendix IV contains additional curves illustrating validation for these same type 2 days in 1968.

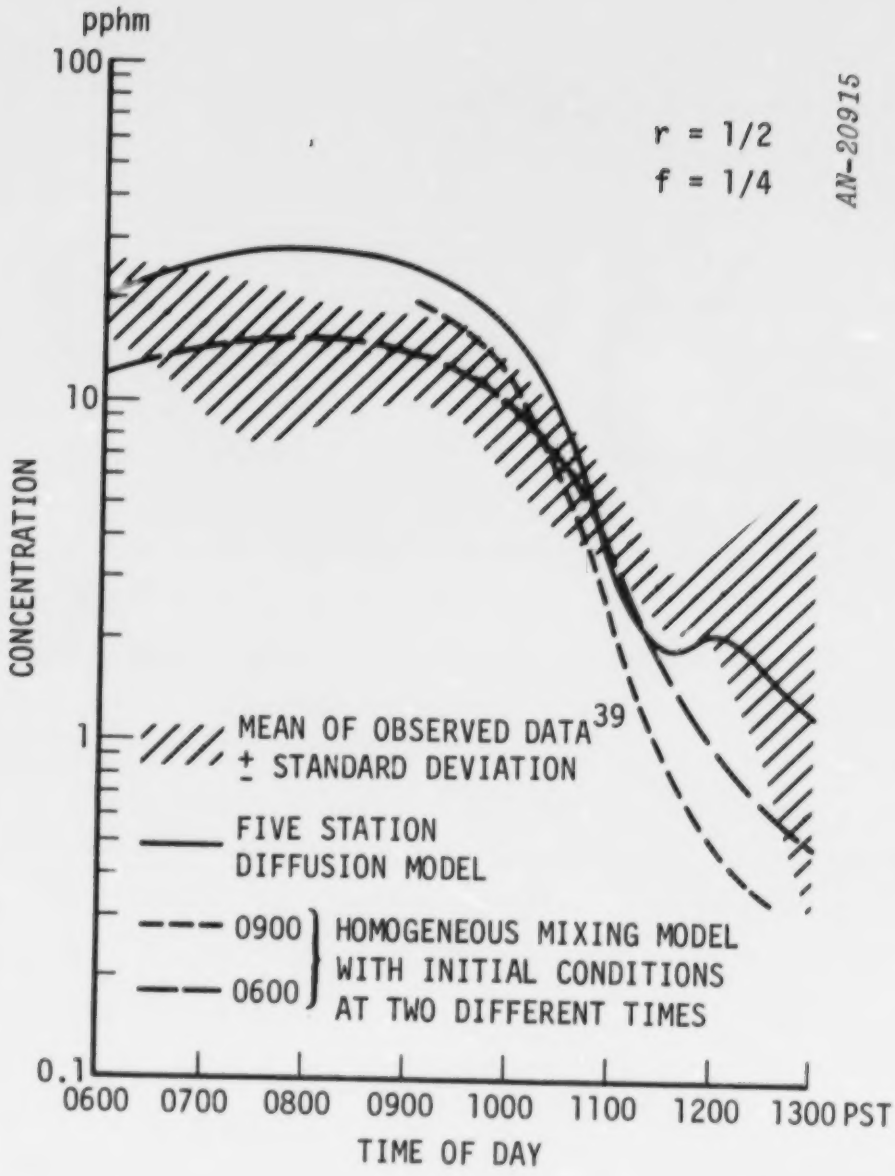

Figure 13. Nitric Oxide Concentration at Huntington Park on Type 2 Day 1968
f = 1/4; r = 1/2

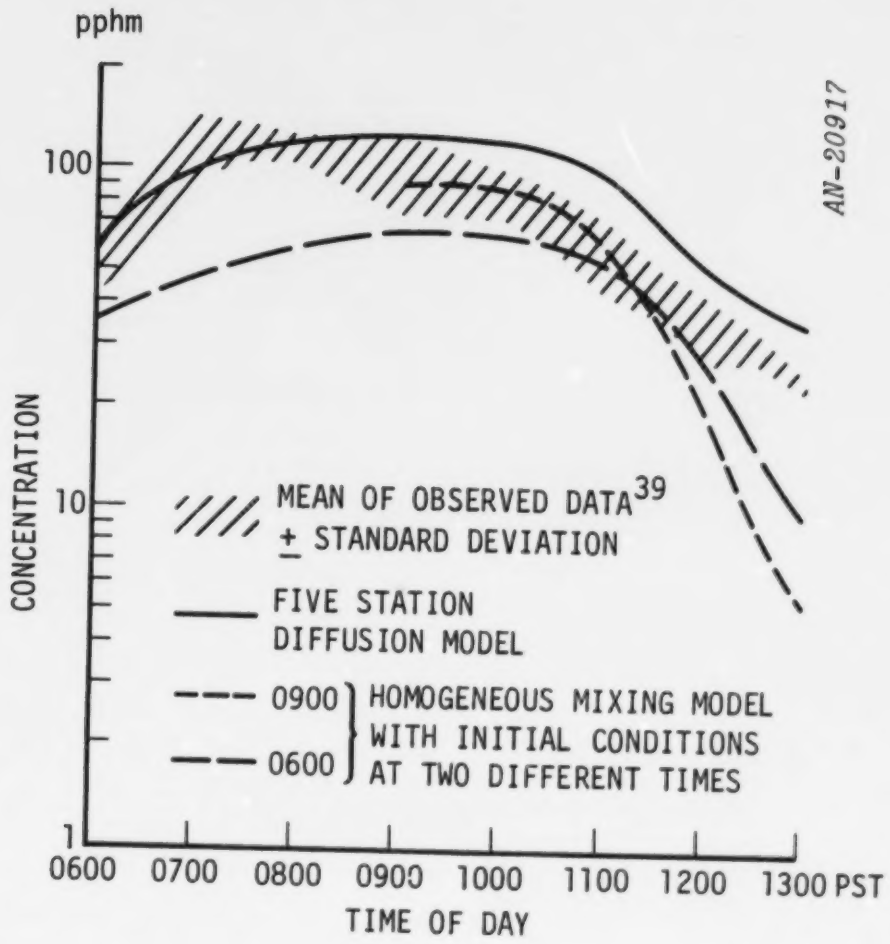

Figure 14. High Reactivity Hydrocarbon Concentration at Huntington Park on Type 2 Days 1968 f = 1/4; r = 1/2

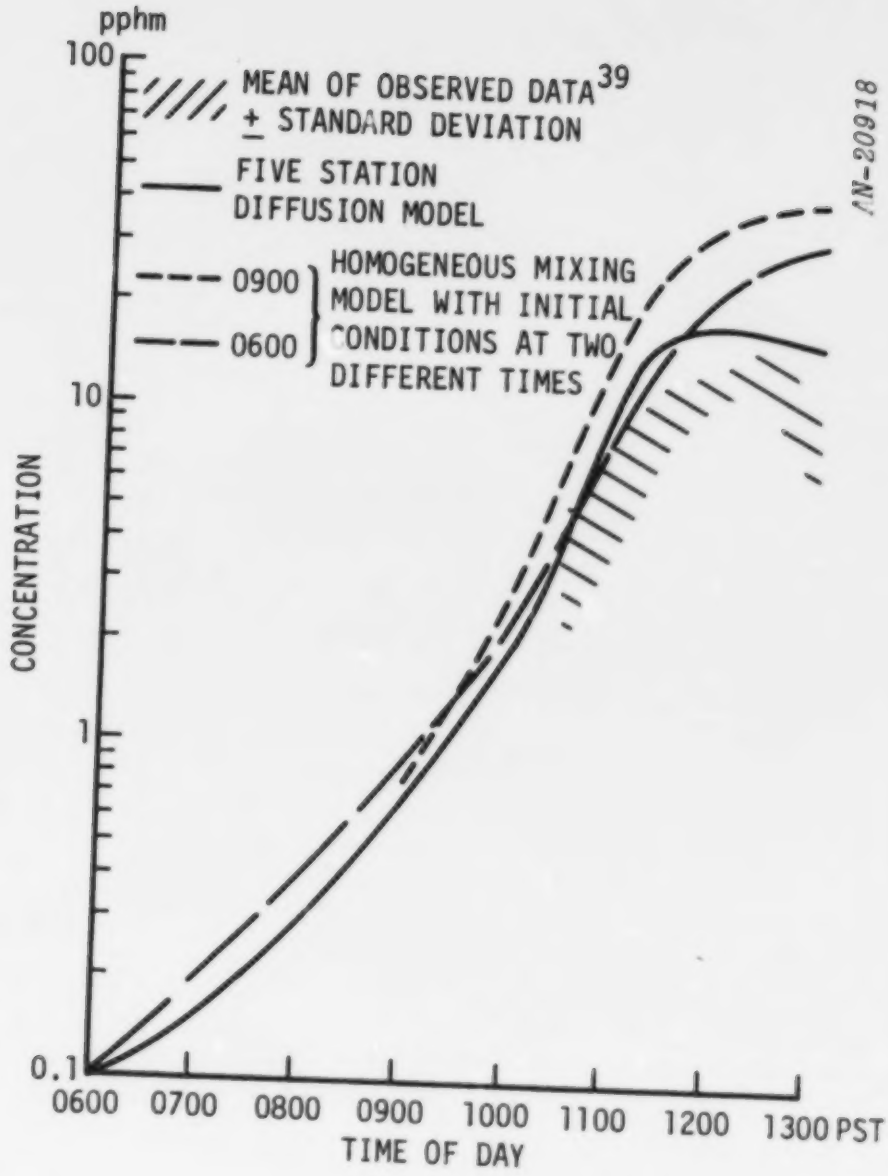

Figure 15. Ozone Concentration at Huntington Park on Type 2 Days 1968
f = 1/4; r = 1/2

IV. CONCLUDING REMARKS

The compelling requirements to relate air quality to specific sources have promoted development of mathematical air pollution models. Our model combines photochemistry with atmospheric transport. The overwhelming complexities of the phenomena coupled with limitations on measurement data have suggested a semi-empirical approach. As laboratory science and theoretical understanding are refined, improved values of coefficients can be introduced into the model calculations.

One area which should be investigated in future work with the model is the low oxidant day. The scope of the present work has been limited to type 2 and 3 days, but further efforts should be directed to data analysis or modeling for types 0 and 1 days. The full range of atmospheric response to the primary pollutants must be mapped out to ascertain how much hydrocarbon or NO_x control is necessary to bring oxidant levels within ambient air quality standards.

Gross meteorological data, laboratory chemistry information, and source inventory estimates have combined to give encouraging results in the model calculations for the Los Angeles basin. While the scope of the problem seems narrow in the investigations made heretofore, numerous questions of a basic nature have been brought to light. For example, it seems desirable now to study interactions in hydrocarbon mixtures having widely differing reactivities in chamber experiments (e.g., Ref. 43). Other experiments are being directed at studying the distribution of nitrate compounds from polluted air in an effort to solve the nitrogen balance.

The present work has demonstrated that composition changes can be described using finite difference calculations of reaction kinetics coupled with atmospheric transport processes. Validation results for the major smog episode in Los Angeles in 1968 are realistic in tracing hydrocarbons, oxides of nitrogen, and ozone. Present deviations from

observations are likely to be explained by imprecision in the large variety of inputs. There is a good basis for expecting these to be resolved within existing instrumental techniques and within practical limits of computer capability.

The future of the mathematical modeling techniques is linked to cooperative activity between the theoretical and experimental arts in the field of air pollution. Phenomena of importance are yet to be added to any of the mathematical schemes. The formation of aerosol and its extinction of ultraviolet radiation has not been explicitly treated in the computations. Moreover, the whole area of heterogeneous reactions on either particulate surfaces or urban surfaces remains obscure. The reacting flow problem of mixedness and its influence on kinetics has not been reduced to an engineering procedure for calculational purposes.

Urgent needs for improved air quality management demand renewed vigor in our attack on many of the fluid dynamic and chemical kinetic areas plagued by chronic difficulties. Turbulent mixing and free radical processes play significant roles here as in many previous technical problems. Pragmatic perspective must guide us, however, in the development of mathematical modeling lest it become a prophecy which fulfills itself in totally abstract research activity.

APPENDIX I

FURTHER VALIDATION TESTS USING CHAMBER DATA

A. INFLUENCES OF COMPOSITION AND LIGHT INTENSITY

To build confidence in the model for the trans-2-butene/nitrogen oxide system, tests for variations in experimental parameters are useful. In Ref. 16 the effect of raising the initial nitric oxide concentration is examined. For an NO_2 photodissociation rate of 0.2 min^{-1}, the observed hydrocarbon half-life increases from 18 to 30 minutes if the initial NO concentration is raised from 4.2 to 16 ppm. The model displayed an increase of only 18 to 23 minutes for the same change. This suggests that the use of the model should be restricted to HC/NO_x mole ratios in the vicinity of 10/4.2 where validation is done. Fortunately, the polluted atmosphere concentration ratios are in this vicinity for cases of interest.

Another composition test is the substitution of NO_2 for NO as an initial reactant with trans-2-butene. Figure 16 shows the results of this test. Curve (c) for the NO_2 runs agrees best with the experimental observations, but the ozone-hydrocarbon rate coefficient had to be decreased from 0.6 to 0.08 $ppm^{-1}min^{-1}$. As seen from Table 1 of the body of this paper, the latter value is still within the bounds given in the review article of Altshuller and Bufalini.[12] Repeated PHOKIN trials showed that the dash curves of Fig. 16 are practically unaffected by plausible variations of the O-atom/hydrocarbon rate coefficient. Furthermore, only late time behavior is influenced by variations in the RCO_x/NO_2 rate coefficient. Evidently the experiment is indicative of the ozonation rate of trans-2-butene because of the insensitivities to others.

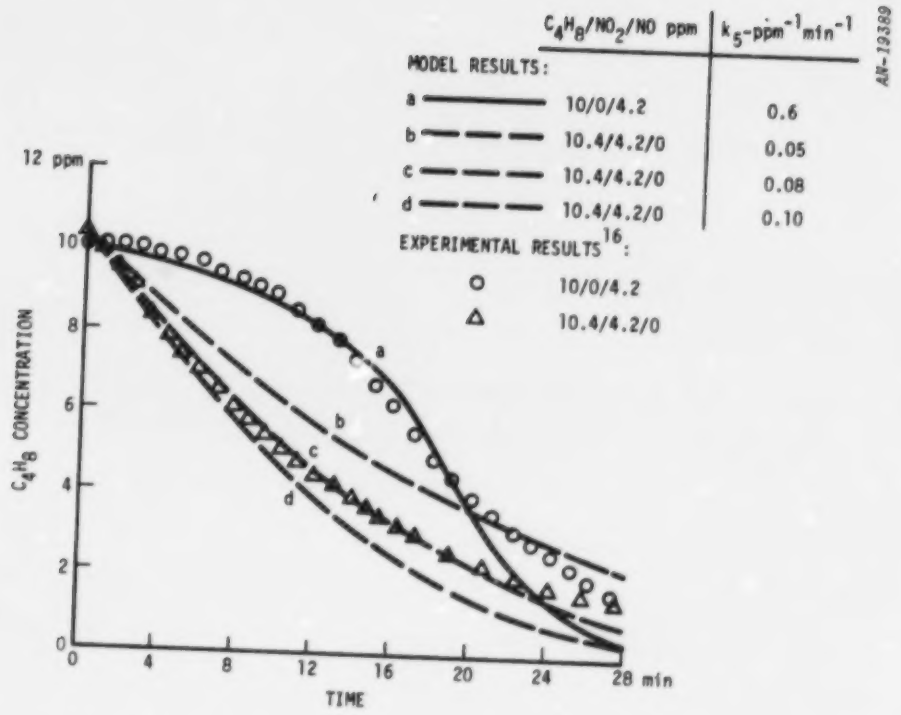

Figure 16. Influence of Nitrogen Oxide on Trans-2-Butene Photo-oxidation for $k_1 = 0.20$ min^{-1}

The disparate findings reported previously for the ozone/hydrocarbon rate coefficient suggest a mechanism far more complex than the single step which is assumed. An attempt to use $k_5 = 0.08$ ppm^{-1}min^{-1} for the conditions of Figs. 2 and 3 gives good modeling for the first 5 minutes, but all concentrations begin to lag observations seriously beyond this point. It is possible that experimental work will be necessary to resolve the uncertainty in this reaction rate.

Another test parameter at our disposal is the light intensity which sets the level of the NO_2 photodissociation rate expressed by k_1 or k_9. Continuing with the results of Tuesday's experiments,[16] we find rather good modeling of both the 20 and 50 percent oxidation times as shown on Fig. 17. On the other hand, the computed times for 80 percent oxidation fall anywhere from 8 to 25 percent short of the observations. This may be another indication that the ozone/trans-2-butene rate is overestimated, but the compromises necessary to model successfully in Figs. 2 and 3 preclude further reductions of k_5.

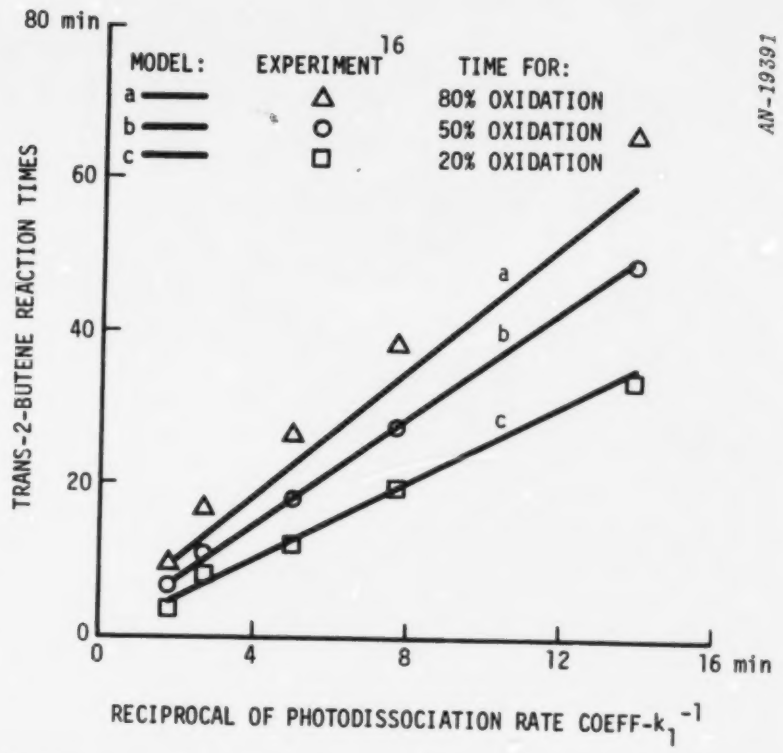

Figure 17. Influence of Light Intensity on Trans-2-Butene Photo-oxidation (Initial Concentrations: (C_4H_8/NO) = (10/4.2 ppm))

B. EXTENSION TO PROPYLENE/NITRIC OXIDE SYSTEM

Following the same procedure as before, we choose a set of nominal values for rate coefficients and try to find a plausible set of adjustments to model a specific irradiation chamber experiment. The data base for this case is obtained from the findings of Altshuller et al.,[22] which are reported in the literature. Table 3 supplies the nominal and validation values for the rate coefficients used to obtain the results plotted in Fig. 18. Here again we needed an increase in the hydrocarbon oxidation rates to validate the model. This time, the O-atom/hydrocarbon coefficient was boosted by a factor of 7.3 and the ozone coefficient is 50 times greater than the top of the experimentally observed range of values. Curves in Fig. 18 suggest that even larger increases might be appropriate. The ozone producing reaction rate was increased over a factor of 4.

TABLE 3

RATE COEFFICIENTS FOR PROPYLENE/NITRIC OXIDE SYSTEM

Reaction	Nominal Values	Validation Values
$h\nu + NO_2 \rightarrow NO + O$	0.40 min^{-1}	0.40 min^{-1}
$O + O_2 + M \rightarrow O_3 + M$	1.32×10^{-5} $ppm^{-2}min^{-1}$	1.32×10^{-5} $ppm^{-2}min^{-1}$
$O_3 + NO \rightarrow NO_2 + O_2$	21.8 $ppm^{-1}min^{-1}$	21.8 $ppm^{-1}min^{-1}$
$O + C_3H_6 \rightarrow 2.5\ RCO_x + Ald.$	6.80×10^{3} $ppm^{-1}min^{-1}$	4.97×10^{4} $ppm^{-1}min^{-1}$
$O_3 + C_3H_6 \rightarrow 2.5\ RCO_x + Ald.$	9.3×10^{-3} to 1.2×10^{-2} $ppm^{-1}min^{-1}$	1.8×10^{-1} $ppm^{-1}min^{-1}$
$RCO_x + NO \rightarrow NO_2$	$\leq$50 $ppm^{-1}min^{-1}$	50 $ppm^{-1}min^{-1}$
$RCO_x + O_2 \rightarrow 0.5O_3$	$\leq$50 $ppm^{-1}min^{-1}$	2.3×10^{-5} $ppm^{-1}min^{-1}$
$RCO_x + NO_2 \rightarrow 0.67\ PAN$	$\leq$50 $ppm^{-1}min^{-1}$	6 $ppm^{-1}min^{-1}$

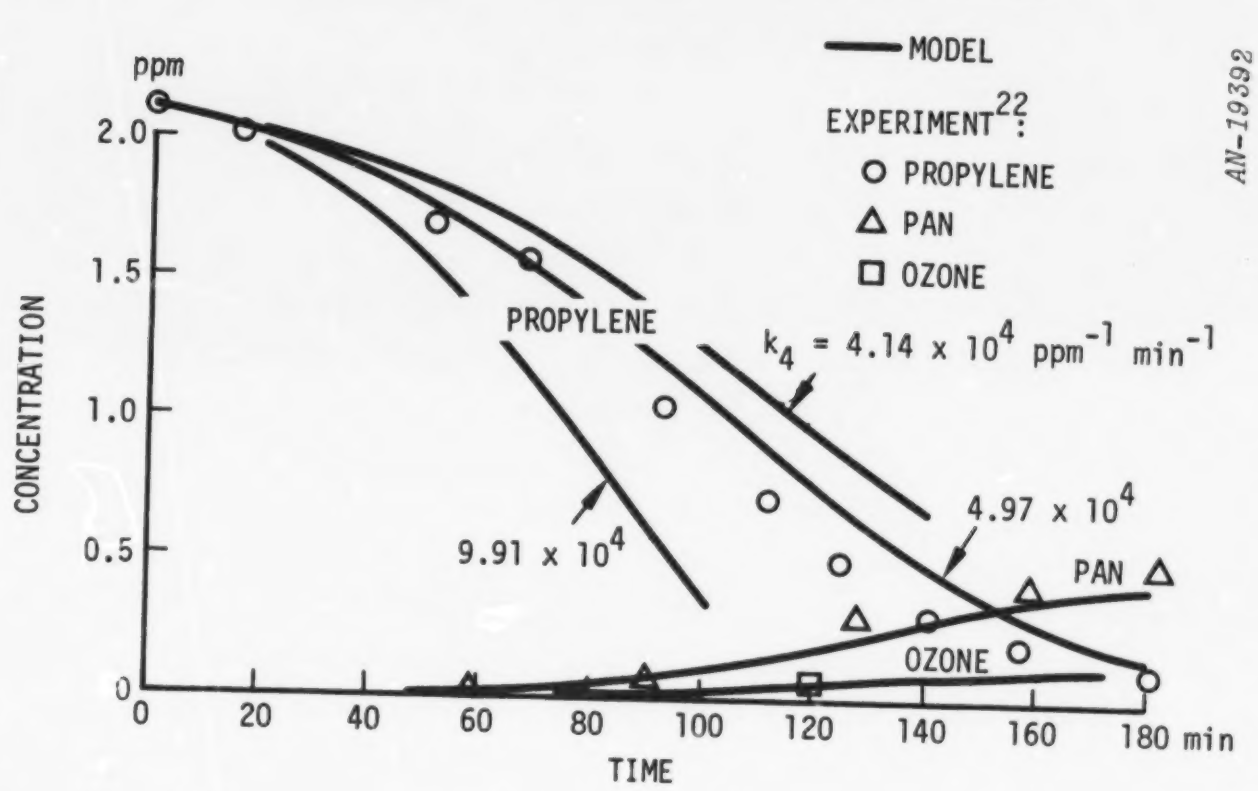

Figure 18. Computed and Observed Composition History (Rate Coefficients in Table 3

Propylene is somewhat more reactive than the average mix of hydrocarbons in automobile exhaust, but it is much closer to automobile exhaust than trans-2-butene.[21] Ethylene is one of the best simulators of hydrocarbon oxidation rate; however, there is little or no PAN produced in its photo-oxidation with nitric oxide.[12] Further extensions of the model to other hydrocarbon/nitrogen oxide systems should be possible by adjusting coefficients in accordance with observed behavior.

APPENDIX II

FINITE DIFFERENCE EQUATIONS FOR THE MODEL

We write the governing equation as a finite difference expression in the three-dimensional grid shown in Fig. 19. The zt-plane is the DIFKIN grid and we have added the zx-plane for horizontal advection. The wind speed u must be given as an input from meteorological data.

In the zt-plane, the typical field difference equation is based on using data at time step m to find out what things become at step $m+1$ at a time τ later). The typical field difference equations for species j is as follows:

$$-\frac{D}{2\xi^2} c_{jm+1,n-1} + \left(\frac{1}{\tau} + \frac{D}{\xi^2} + \frac{P_{j,m,n}}{c_{j,m,n}}\right) c_{j,m+1,n} - \frac{D}{2\xi^2} c_{jm+1,n-1}$$

$$= \frac{D}{2\xi^2} (c_{j,m,n+1} + c_{j,m,n-1}) + \left(\frac{1}{\tau} - \frac{D}{\xi^2}\right) c_{j,m,n} + R_{j,m,n} - P_{j,m,n} + Q_{j,m,n,k}$$

$$\text{For} \begin{Bmatrix} j = 1, 2, 3, \ldots s \\ n = 1, 2, 3, \ldots p \\ k = 1, 2, 3, \ldots q \end{Bmatrix} \qquad (2)^*$$

where

$$R_{j,m,n} = (m_j/m) \sum_{i=1}^{r} \beta_{ij} k_i \prod_{\lambda=1}^{s} (mc_\lambda/m_\lambda)^{\nu_{i\lambda}} \qquad (3)$$

$$P_{j,m,n} = \frac{1}{2} \sum_{i=1}^{r} \nu_{ij} R_{ij,m,n} \qquad (4)$$

---

*The subscript k indicating the x-direction grid points should be understood to apply to each species concentration in these equations. It has been omitted for clarity. Equation 5 however, treats the horizontal advection term and has the full subscripting.

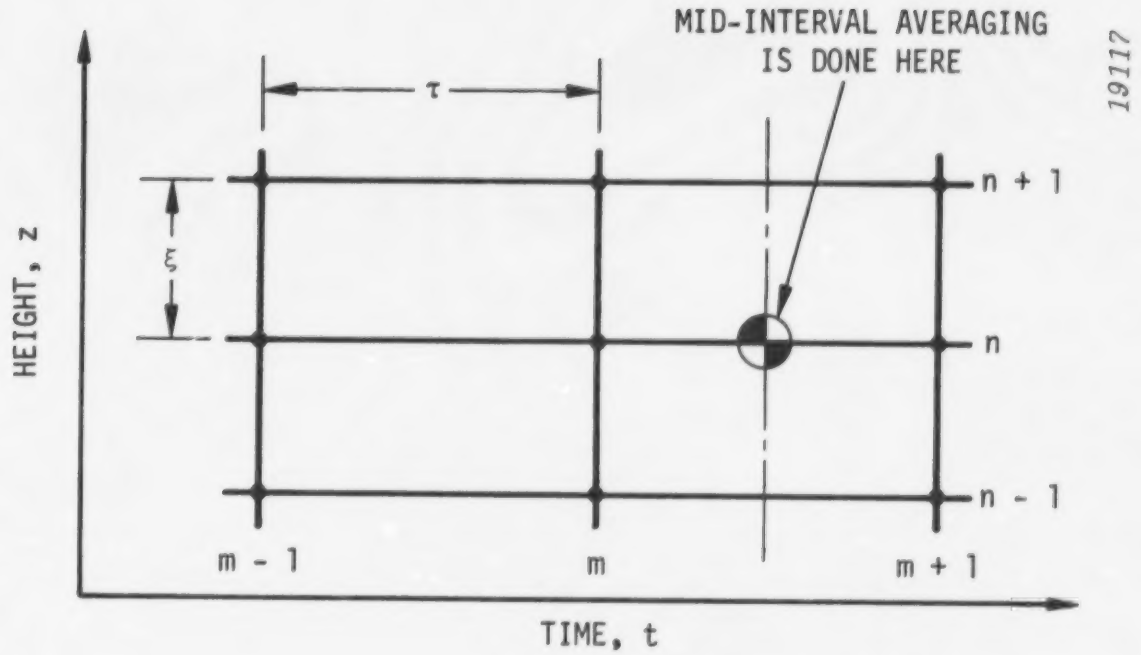

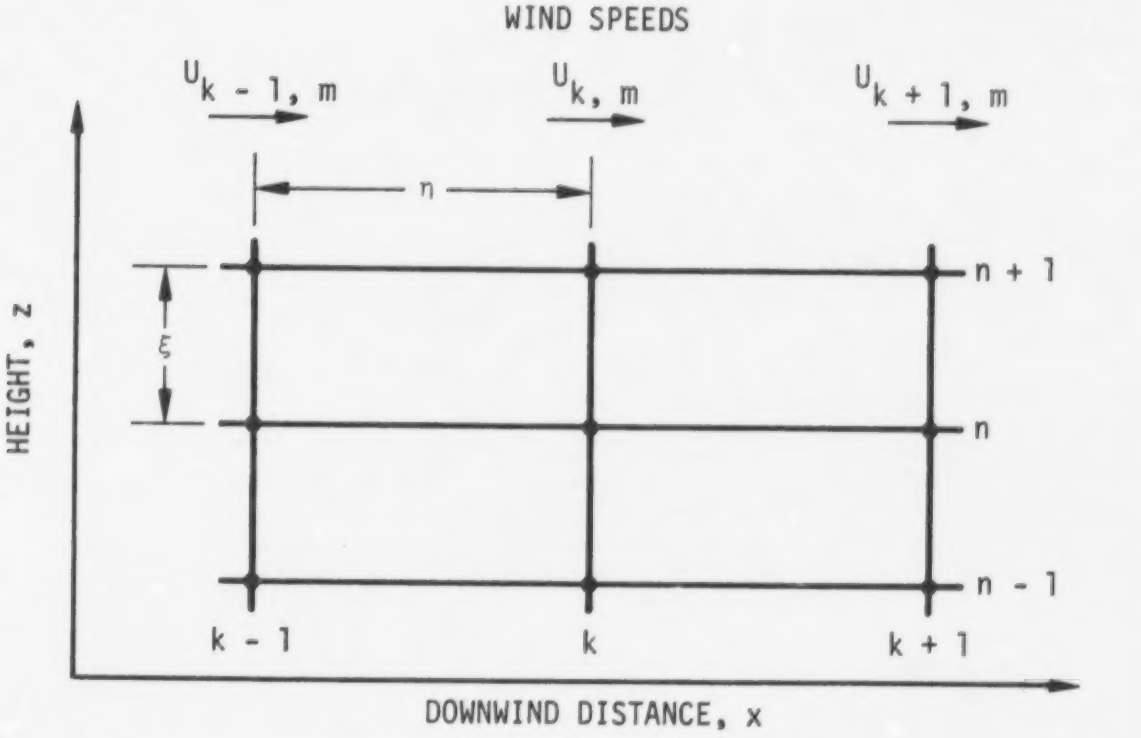

Figure 19. Three-Dimensional Calculation Grid

and for $k < q$

$$Q_{j,m,n,k} = \frac{1}{2}\left[\left(\frac{u_k + u_{k-1}}{2}\,\frac{c_{j,k} - c_{j,k-1}}{\eta}\right)_{m,n} + \left(\frac{u_{k+1} + u_k}{2}\,\frac{c_{j,k+1} - c_{j,k}}{\eta}\right)_{m,n}\right] \tag{5a}$$

for $k = q$

$$Q_{j,m,n,q} = \frac{1}{4}\left[(3u_q + u_{q-1})\left(\frac{c_{j,q} - c_{j,q-1}}{\eta}\right)\right]_{m,n} \tag{5b}$$

where m_j = molecular weight of jth species

m = molecular weight of mixture

ν_{ij} = reactant j stoichiometric coefficient in reaction i

β_{ij} = net stoichiometry of jth species from ith reaction (i.e., $\beta_{ij} = \nu'_{ij} - \nu_{ij}$)

k_i = rate coefficient for ith reaction

p = number of vertical mesh points

q = number of horizontal mesh points

r = number of reactions

s = number of species

$P_{j,m,n}$ = first-order Taylor series correction to $R_{j,m,n}$ to estimate mid-interval value on first term

ξ,τ,η = intervals of height, time, and downwind distance

The inclusion of the horizontal advection term $Q_{j,m,n,k}$ requires an additional boundary condition, which could take the following form

$$c_j(t,z,x = x_o) = f_j(t,z)$$

where f_j is some known function of time and height at some downwind distance x_o. In the present study we used

$$x_o = 0$$

and

$$f_j(t,z) = \text{constant} \simeq 0$$

For second and higher iterations, we substitute $R_{j,m+0.5,n}$ for $R_{j,m,n}$ and set $P_{j,m,n} = 0$ because we then have $(m+1)$ values to average with. Similarly we substitute time-averaged concentrations and velocities in Eqs. 5 to get $Q_{j,m+0.5,n,k}$ for the mid-interval averaged convective flux for the jth species. Since there are s species and r reactions, the typical (ith) chemical reaction step is represented by

$$\sum_{j=1}^{s} \nu_{ij} M_j \rightarrow \sum_{j=1}^{s} \nu'_{ij} M_j \qquad ; \quad i = 1, 2, 3, \ldots r \tag{6}$$

The symbol M_j is the chemical formula of the jth species.

From this we see that at each (kth) location in the basin along the wind path we have a way of integrating with time the species equation by knowing concentrations at each (mth) time step. The left-hand side of Eq. 2 is in terms of prescribed (but variable) coefficients operating on the unknown concentrations at the next (m+1st) time step. There are as many of these equations as there are species and vertical stations at each horizontal location. The advective aspect is solved round-robin by updating the profile at each horizontal location in time starting from the "fresh air" input from the sea at $k = 1$ and marching downwind to $k = q$.

APPENDIX III

SPECIFICATIONS FOR THE DATA STATISTICAL ANALYSIS PROGRAM

Certain aspects of the Scott data such as gaps and odd times make it awkward to use the raw data for model validation. In order to put the data into a more useful form two computer programs have been developed. These programs are very general in nature and thus may be used with data not peculiar to 1968. The programs are called SORT and SORT1 and their capabilities are described below. A few general comments can be made about both programs, however.

Both programs can handle large quantities of data. However, since it is desirable to use as little core memory as possible for a given job, the programs have been designed so that simple modifications can enlarge the data handling capacity while at the same time optimizing the storage space for a given set of data. The end result is that very little core is left idle and costs are reduced.

SORT

This program carries out the data ordering and smoothing. Given any number of hydrocarbon species whose respective concentrations are measured at arbitrary times, the program computes the concentration of these species at nominal times from 0500 to 1400 PST at 30-minute intervals. These times were chosen to coincide with the end points of the 1968 Scott data and can be easily changed. The algorithm senses gaps in the data and can fill these gaps by uniform extrapolation and linear interpolation. Linear interpolation is used throughout to compute concentrations at the nominal times. To facilitate the preparation of data and to eliminate manual data handling, the program has a built-in data ordering algorithm. The data are grouped by station, date, and time. The computation routines are

considerably simplified by ordering the data in this manner. Using the smoothed data, SORT computes the total concentration for any one of 32 groups of six reactivity classes for a given time for a given station for any number of stations taken two at a time. The average concentration for any specified grouping of reactivity classes for one or two stations is also computed. As an option, weighted and unweighted averages for both stations taken together are calculated. The averages are computed for any number of days specified by the user; the days specified for each station need not be the same. Given an input date, the program searches for that date through the available data; if data for that date is not available, a message is printed and the next date is read. Averages are output at the nominal times.

Some of the output of SORT is output in the form of punched cards and/or magnetic tape. This output is then used as input for SORT1. The form of the output is optional with the user. Quantities output in this way are:

1. Interpolated concentrations for each species for each station (input for SORT1)
2. The data ordered by station and date
3. Data stating the number of interpolated quantities at a given station on a given date (input for SORT1)

The data ordered by station and date is stored on magnetic tape for future use. This ordering is constant for a given data set and need only be carried out once and then used as input in successive runs.

As an added feature, SORT outputs a catalogue of all the dates requested by the user classified according to type, i.e., type 0, 1, 2, 3. This output is further subdivided into groups detailing the dates that were found in the available data and the dates missing from the data.

Each of these date groups is also classified by type. The dates on which only a single time reading was present are presented as a separate group. This catalogue is intended to give the user an idea of the amounts and kinds of data available.

INPUT/OUTPUT SPECIFICATIONS FOR DATA PREPARATION PROGRAM

Inputs in the order used in the data deck

1. Name, identification number, carbon number, reactivity index, and molecular weight of each species: These are stored in three arrays:

   a. Name is stored in array ANAME

   b. Identification number, carbon number, and reactivity index are stored in columns 1, 2, 3 respectively of array ID

   c. Molecular weight is stored in array WTMOLE.

   Each species has all the information on one card in the following fashion:

Columns	1-10	1-15	16-20	21-25	26-30	31-35	36-46
	Name	Blank	ID No.	Blank	Carbon No.	Reac-tivity Index	Molecular Weight

   The format is (A10, 5X, I5, 5X, 2I5, F10.3)

2. The name of each station: There are eight stations and their code names are:

   a. HUNTPARK
   b. EL MONTE
   c. STADIUM
   d. WHITEAIR
   e. LA CANADA
   f. EVERGREEN
   g. GRAVELPIT
   h. SANTAFEDAM

   There are stored in array STATION. HUNTPARK and EL MONTE must be the first and second elements of STATION respectively. Each name is entered on columns 1-10 of a card, one name to a card. The format is (A10). The station identification number is the number of the position of the station in the above list.

3. The name of the station to which the data to be read corresponds: This variable is called TITLE in the code. The format used is the same as for STATION.

4. The number of data cards to be read for the station in question: This is called NDATA in the code.

5. The input dates for the station in question: The dates are grouped together and are read sequentially by the code. That is, the first date is read and all the computations are carried out for that date. The second date is then read and the process is repeated. There can be any number of cards in the date deck for a station. The information required on each card is the following:

COLS	1-5	6-10	11-15	16-20
	STATION IDENTIFICATION NUMBER (HUNTPARK - INDO = 1) (ELMONTE - INDO = 2)	MONTH	DAT	TYPE OF DAY (Type 2, 3, etc.)

The format used is (4I5)

After the last date card one must insert a card containing a negative integer in columns 1-5. This is an indicator for the program to know that no more dates are forthcoming.

On the other hand, if more dates for a second different station are to be read then a negative integer must be punched in columns 6-10.

A sample input deck is depicted on the next page. (Fig. 20)

6. The subpopulation descriptors: This information is contained on one card as follows:

COLS	1-5	6-10	11-15, 16-20, 21-25, 25-30
	No. of SUBPOPULATIONS (1,2,3,4,5,6)	No. of Reactivity classes in SUBPOPULATION NO. 1	Same as columns 6-10 for each of five other SUBPOPULATION groups.

The format used is (6I5).

SAMPLE INPUT DECK

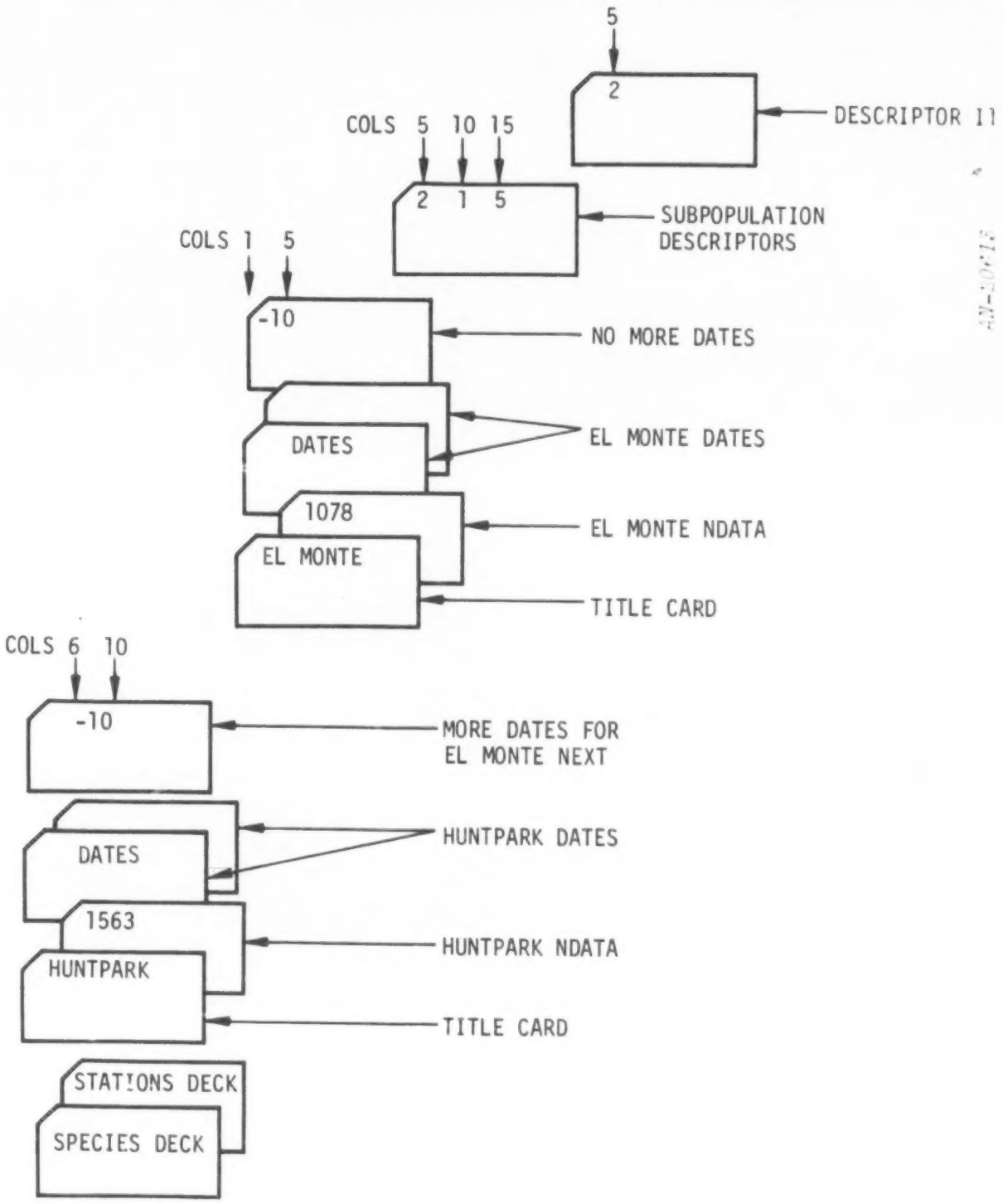

Figure 20. Sample Input Deck

The number of subpopulations is stored in variable NPOP. If NPOP = 6 the other entries may be left blank. Example: two subpopulations, the first one with reactive class 1 (inert) and the second one with the remaining five reactivity classes. The card would read:

COLS	5	10	15	16-30
	2	1	5	Blank

7. A descriptor, I1 in the code, which determines whether the averages for one or two stations are to be computed: If I1 = 1, the integer 1 punched in column 5, the averages for only one station are computed. If I1 = 2 the averages for both stations are computed.

COLS	5
	1
	(2)

Outputs

I. Printed (in the order of appearance)

1. Input data

   a. Species name, identification number, etc.

   b. Title, number of species, number of data cards, number of reactive classes

   c. The concentration for each species along with the station where measured and date and time when measured

   d. The data in (c) above after ordering by date and station

   e. The data in (c) for a particular day ordered by time

2. Interpolated concentrations for each species and time

3. The totals for each reactivity class

4. The totals for each subpopulation

5. The average concentrations for each station

6. The average concentrations for two stations taken together (both weighted and unweighted averages)

7. Catalogue of dates specifying the dates present and missing from the available data

II. Punched and/or Tape Output

1. The interpolated concentrations

2. Data specifying the number of interpolated quantities for a given station on a given date

3. Data ordered by date and station (one time only for a given data set)

SORT1

SORT1 utilizes the interpolated quantities from SORT, read in either from magnetic tape or punched cards, and computes weighted averages for reactivity, carbon number, and molecular weight for any one of 32 subpopulations of hydrocarbons grouped according to reactivity class. The standard deviations for these averages as well as for the average concentration of each group are also calculated. Averages for reactivity, carbon number, and molecular weight are provided in three forms.

1. Averages for each time for a single day
2. Weighted averages for each time for all days (each day weighted according to the total concentration on that day)
3. Unweighted averages for each time for all days (all days with equal weight, weight = 1).

SORT1 also has the capability of subdividing the species into subpopulations according to reactivity class independently of SORT. This provides greater flexibility in the use of SORT1.

The equations used in the computations are the following:

Let m_{ij} = mole fraction of the ith species at a given time on the jth day

X_i = specific reactivity, carbon number, molecular weight of the ith species

n_j = number of species present on the jth day at a given time

$\bar{X}_j$ = average specific reactivity, carbon number, or molecular weight at a specific time on the jth day

$\bar{\bar{X}}_w$, $\bar{\bar{X}}_u$ = weighted and unweighted average specific reactivity, carbon number, molecular weight at a given time for all days

σ = standard deviation

$$M_j = \sum_{i=1}^{n_j} m_{ij} = \text{total mass fraction for a subpopulation containing } n_j \text{ species on the } j\text{th day}$$

N = the total number of days

Then

$$\bar{X}_j = \frac{\sum_{i=1}^{n_j} m_{ij} X_i}{\sum_{i=1}^{n_j} m_{ij}}$$

$$\bar{\bar{X}}_u = \frac{\sum_{j=1}^{N} \bar{X}_j}{N}$$

$$\bar{\bar{X}}_w = \frac{\sum_{j=1}^{N} M_j \bar{X}_j}{\sum_{j=1}^{N} M_j}$$

$$\sigma_u = \left[\frac{\sum_{j=1}^{N} (\bar{X}_j - \bar{\bar{X}}_u)^2}{N} \right]^{1/2}$$

$$\sigma_w = \left[\frac{\sum_{j=1}^{N} M_j (\bar{X}_j - \bar{\bar{X}}_w)^2}{\sum_{j=1}^{N} M_j} \right]^{1/2}$$

SORT1 Input/Output

Inputs in the order used in the data deck

1.,2. Same as 1 and 2 for SORT

3. Subpopulation descriptors, same as 6 for SORT

4. Data specifying the station, date, and number of interpolated quantities (output from SORT). The data is stored in an array called INTDAT and the format is (I20).

5. The interpolated quantities corresponding to each entry of INTDAT. May be read in from punched cards or tape.

Printed Outputs - in order of appearance

1. Averages and standard deviations for each station for each time for each day

2. Unweighted averages and standard deviations for each station for each time for all days

3. Weighted averages and standard deviations for each station for all days

APPENDIX IV

ADDITIONAL SPECIES CONCENTRATION GRAPHS

Space limitations and clarity suggest the separation of the remainder of the species graphs for type 2 and type 3 day calculations from those in the main text.

Figures 21, 22, and 23 show additional results for the modeling runs of the type 3 day. Nitric oxide, like high-reactivity hydrocarbons, seems to go from the higher to lower reactivity curves as time progresses. Fig. 22 shows the peak nitrogen dioxide concentration predicted to be some 40 percent below the highest value recorded by SRL. The reactivity shift from $r = 1$ to something less than $r = 1/2$ is exhibited here once more. PAN concentrations on Fig. 23 are probably too high because the nitrate stoichiometry from chamber experiments was retained. As measurements become more numerous, this condition will be reflected more accurately in the model specification.

Type 2 days are plotted on Figs. 24, 25, and 26. Carbon monoxide and low reactivity hydrocarbons show clearly the effects of wind-driven ventilation. Although the data scatter more at late times, a decided downtrend is noticeable. The DIFKIN model is incapable of describing this, but the TADKIN version includes the advection effects. Peaks in the NO_2 curves are underpredicted in magnitude and their time of appearance is overestimated by the model. Measured data peak at 1000 hours on the average, and the predicted curves peak at 1030 to 1100 hours. The same reservations expressed above apply to the PAN curves here.

Figures 27 and 28 show calculations for type 2 days displayed using a new plotting capability at Compucenters, Inc. (a GRC affiliate).

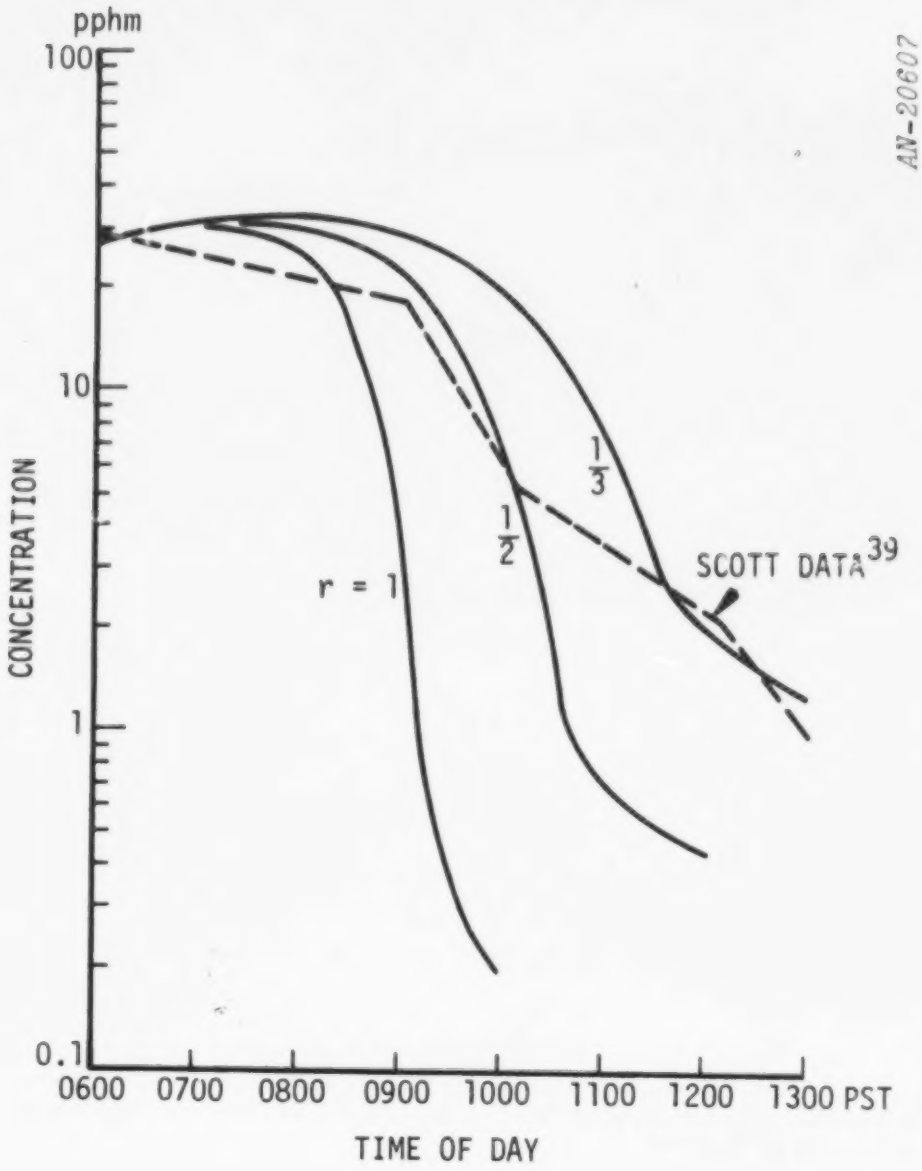

Figure 21. Nitric Oxide Concentration on Type 3 Day; f = 1/4

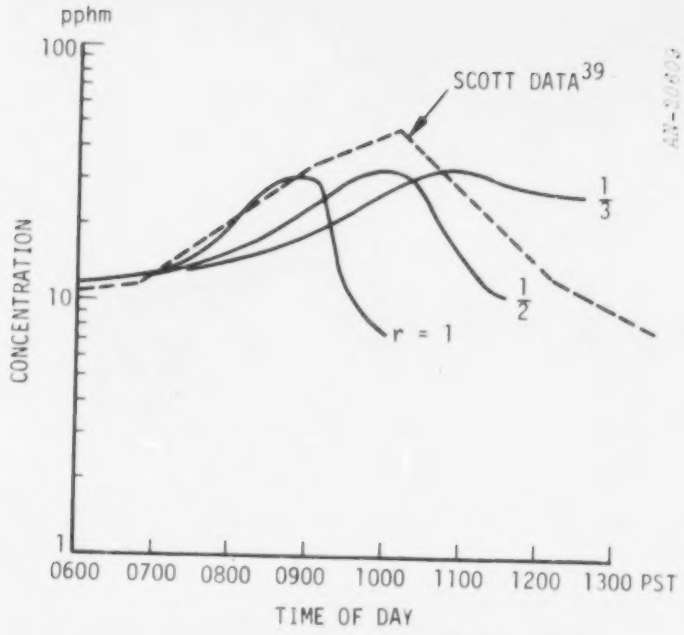

Figure 22. Nitrogen Dioxide Concentration on Type 3 Day; f = 1/4

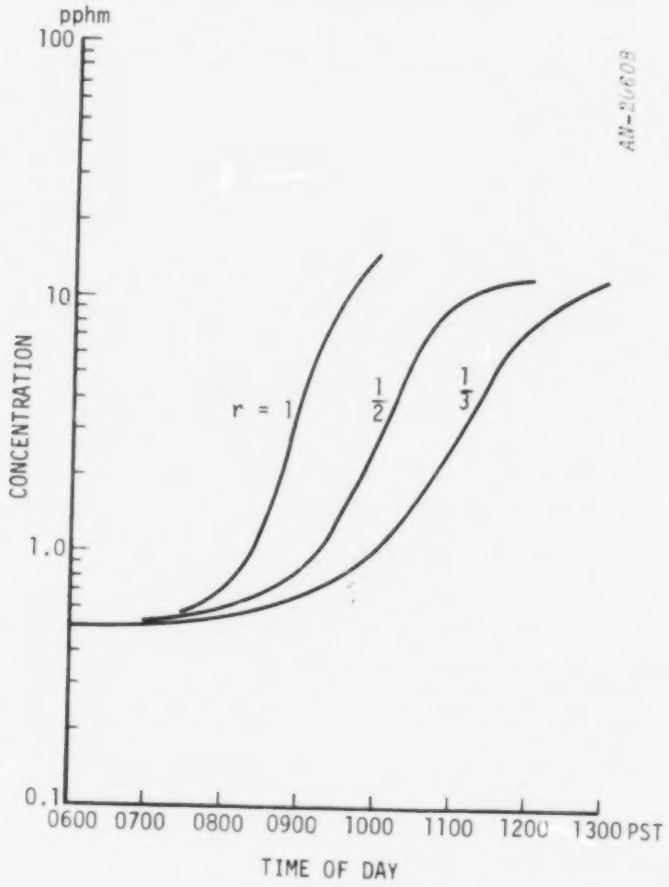

Figure 23. Pan Concentration on Type 3 Day; f = 1/4

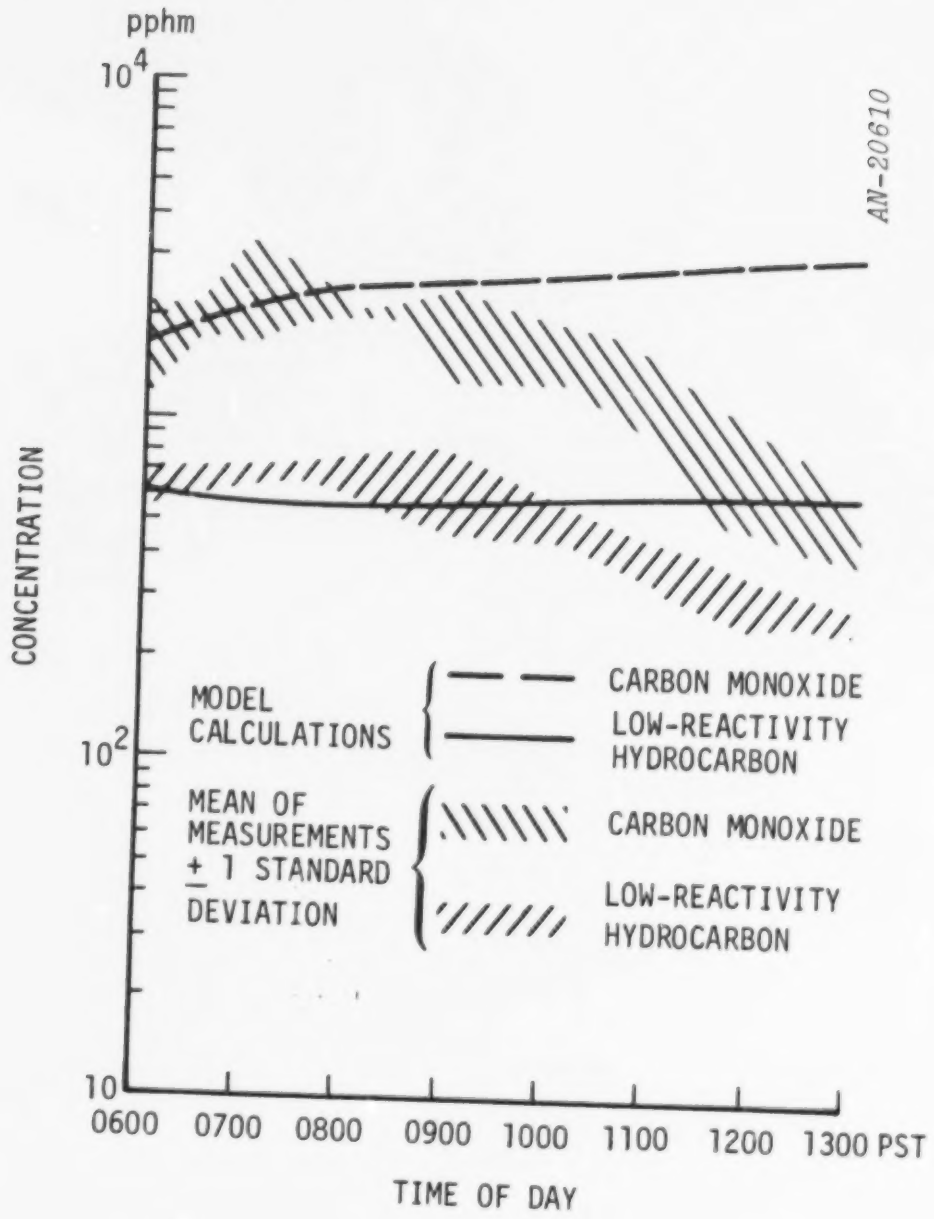

Figure 24. Low Reactivity Hydrocarbon Carbon Monoxide on Type 2 Days 1968 at Huntington Park

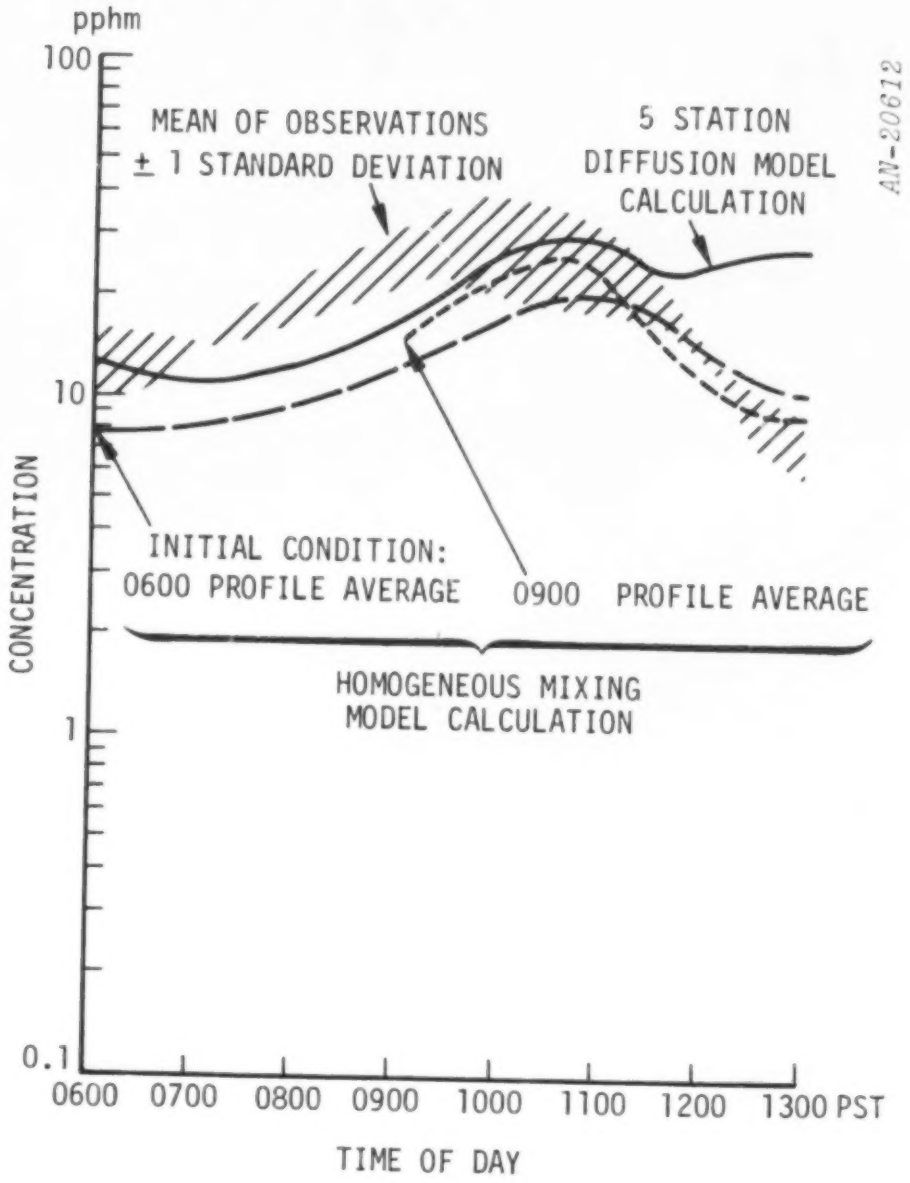

Figure 25. Nitrogen Dioxide Concentration on Type 2 Days in 1968 at Huntington Park

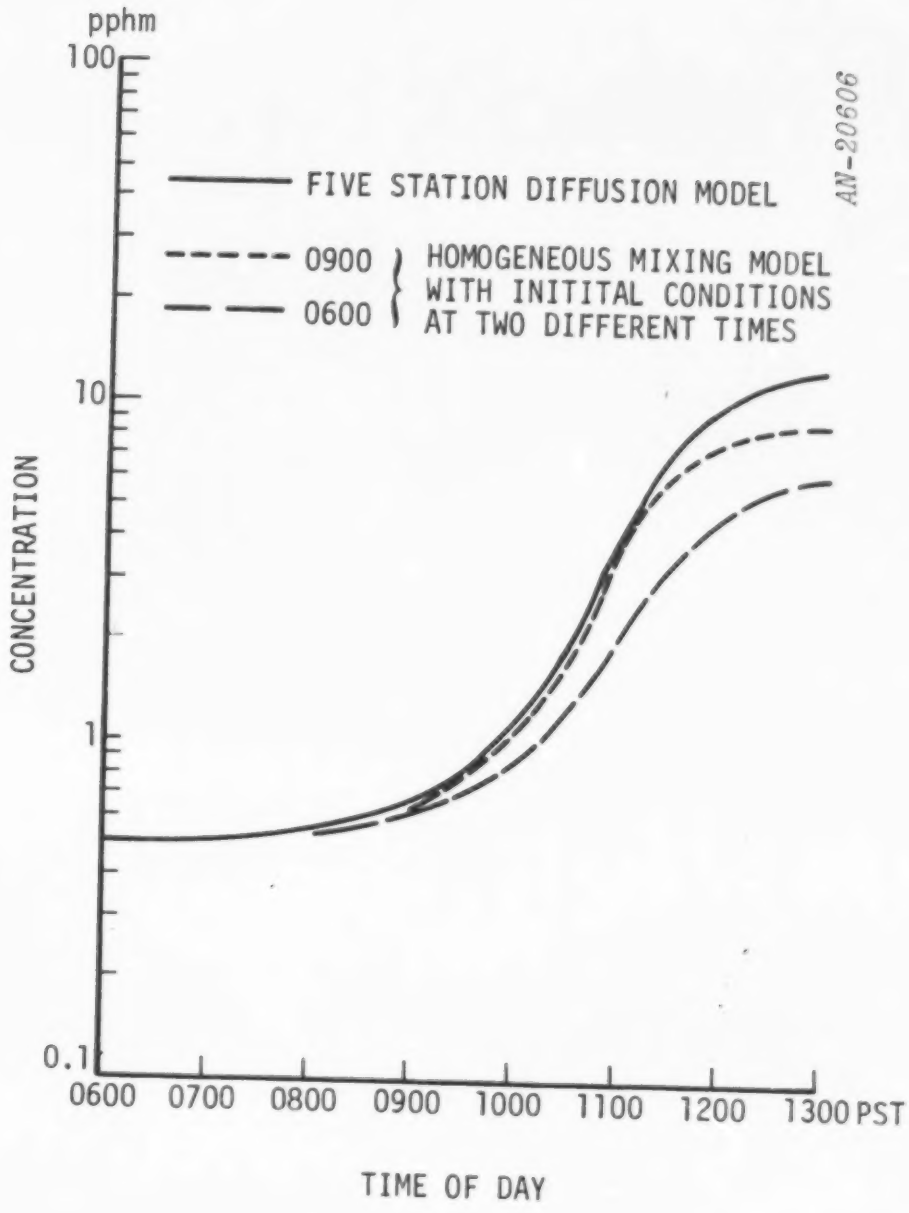

Figure 26. Pan Concentration on Type 2 Days in 1968 at Huntington Park

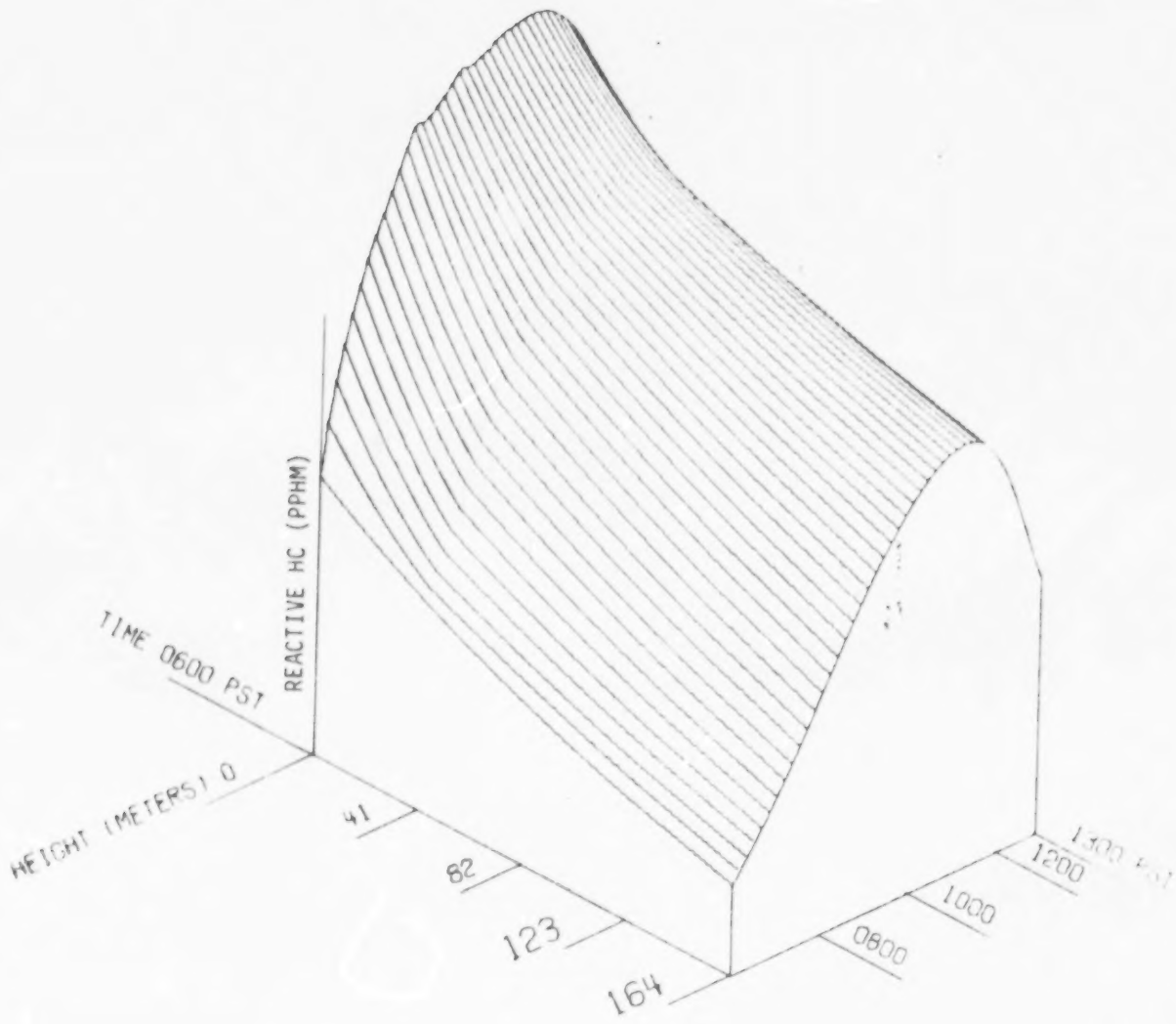

Figure 27. Three Dimensional Plot of High Reactivity Hydrocarbon
f = 1/4; r = 1/3

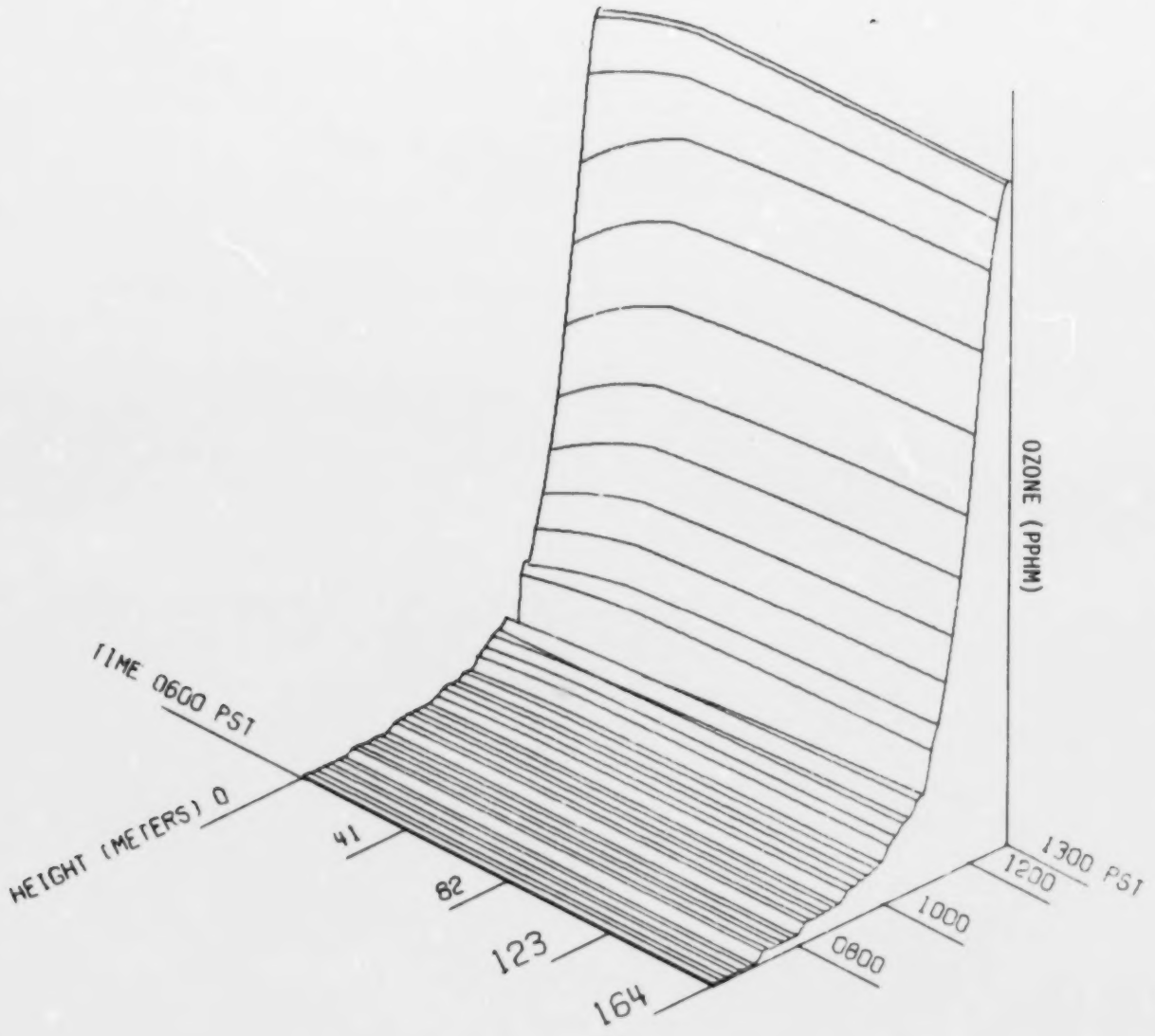

Figure 28. Three Dimensional Plot of Ozone f = 1/4; r = 1/3

APPENDIX V

EL MONTE REACTIVITY INDEX

As reported previously, the reactivity patterns for hydrocarbons measured at El Monte scattered widely. Numerical data processing was carefully checked and no errors were detected. The same preprocessing algorithm was employed to obtain Fig. 9 which exhibits far more regularity.

During a recent field trip to Los Angeles, Mr. Zenophon Tomaras of Scott Research Laboratories supplied much useful information regarding hydrocarbon interferences. Centerline striping operations on nearby streets caused noticeable excursions which were duly noted in the field log. It was suggested that the log notes are essential in evaluating the data for validation use.

These warnings stimulated an inspection trip of the surrounding area. El Monte airport is situated in a sub-basin formed by Rio Hondo Wash and the instrument site is on a small knoll generally on the downwind side of the apron. Dozens of business and utility aircraft are evidently fixed-based at El Monte. It might be expected that frequent handling of Avgas occurs during refueling operations with possible vapor accumulations in the sub-basin. Wind mixing disperses cooler air from this sub-basin following sunrise.

Also upwind from the site, but more distant, are two iron foundries with cupolas and a glass fiber manufacturing plant with a tall stack. All of these industrial facilities were in operation at the time of inspection.

All of these factors raise questions regarding sporadic interference with air composition measurements employing highly sensitive instruments.

Activities likely to cause interference were not observed at either the Commerce (1969) site or the Huntington Park (1968) site; however, some rendering plant emissions were sometimes suspected at the Commerce site.

Because of unanswered questions surrounding the El Monte data, emphasis was placed on analyzing the Huntington Park data in the limited time available. It is entirely possible that internal consistency checks can be devised for assessing interference effects. Since there are only two sites in the program, pursuit of this effort is certainly a fruitful endeavor.

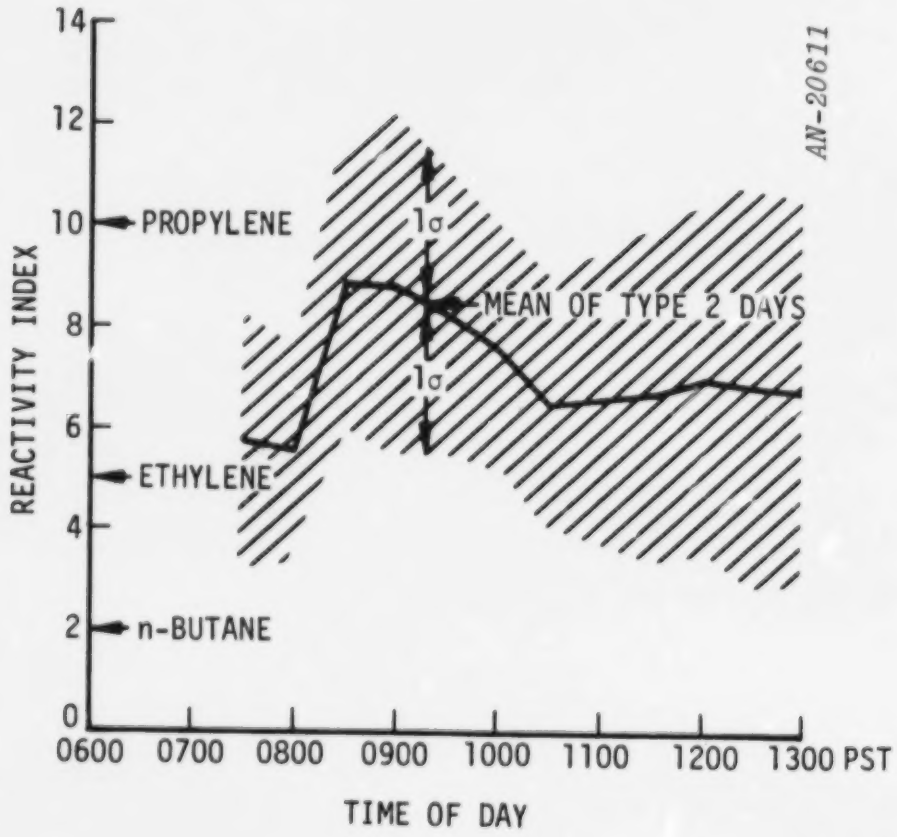

Figure 29. Hydrocarbon Reactivity at El Monte During the Late October 1968 Smog Episode (Same Assumptions as Those Listed on Figure 9)

REFERENCES

1. O. G. Sutton, "A Theory of Eddy Diffusion in the Atmosphere," Proc. Roy. Soc., A, Vol. 135, pp. 143-165, 1932.

2. D. B. Turner, "A Diffusion Model for an Urban Area," J. Appl. Met., Vol. 3, pp. 83-92, 1964.

3. D. B. Turner, Workbook of Atmospheric Dispersion Estimates, U.S. DHEW Environmental Health Series, Cincinnati, Ohio, p. 36, 1967.

4. R. C. Wanta, "Meteorology and Air Pollution," Ch. 7 in Air Pollution (A. C. Stern, ed.) Vol. I, Second Edition, Academic Press, New York, 1968.

5. F. N. Frenkiel, "Atmospheric Pollution in Growing Communities," Smithsonian Inst. Annual Report, pp. 269-299, 1956.

6. W. J. Karplus, G. A. Bekey, P. J. Pekrul, "Atmospheric Diffusion of Air Pollutants," Ind. and Eng. Chem., Vol. 50, pp. 1657-1660, 1958.

7. R. G. Lamb, An Air Pollution Model of Los Angeles, M.S. Thesis, University of California, Los Angeles, 1968.

8. S. K. Friedlander, J. H. Seinfeld, "A Dynamic Model of Photochemical Smog," Environmental Science and Technology, Vol. 3, pp. 1175-1181, November 1969.

9. P. A. Leighton, Photochemistry of Air Pollution, Academic Press, New York, 1961.

10. B. E. Saltzman, "Kinetic Studies of Formation of Atmospheric Oxidants," Industrial and Engineering Chemistry, Vol. 50, No. 4, pp. 677-682, April 1958.

11. L. G. Wayne, "On the Mechanism of Photo-Oxidation in Smog," Archives of Environmental Health, Vol. 7, No. 8, pp. 113-123, August 1963.

12. A. P. Altshuller, J. J. Bufalini, "Photochemical Aspects of Air Pollution: A Review," Photochemistry and Photobiology, Vol. 4, pp. 97-146, 1965.

REFERENCES (Cont.)

13. A. J. Haagen-Smit, L. G. Wayne, "Atmospheric Reactions and Scavenging," Air Pollution, Vol. I, ed. A. C. Stern, Academic Press, New York, 2nd Ed., pp. 149-186, 1968.

14. E. R. Stephens, "Chemistry of Atmospheric Oxidants," J. Air Poll. Control Assn., Vol. 19, pp. 181-185, March 1969.

15. A. Eschenroeder, Validation of Simplified Kinetics for Photochemical Smog Modeling, General Research Corporation IMR-1096, September 1969 (submitted for publication in J. Air Poll. Control Assn.).

16. C. S. Tuesday, The Atmospheric Photo-Oxidation of Trans-Butene-2 and Nitric Oxide, General Motors Research Laboratories GMR-332, 1961.

17. J. J. Bufalini, K. L. Brubaker, Photo-Oxidation of Formaldehyde at Low Partial Pressures, Symposium for Chemical Reactions in Urban Atmospheres, GM Research Laboratories, Warren, Michigan, October 6-7, 1969.

18. A. P. Altshuller, DHEW, private communication, September 1969.

19. K. Westberg, Aerospace Corporation, private communication.

20. E. A. Sutton, "Chemistry of Electrons in Pure-Air Hypersonic Wakes," AIAA Journal, Vol. 6, pp. 1873-1882, October 1968.

21. J. D. Caplan, "Smog Chemistry Points the Way to Rational Vehicle Emission Control, Vehicle Emissions II," SAE Progress in Technology, Vol. 12, New York, pp. 20-31, 1966.

22. A. P. Altshuller, S. L. Kopcaynski, W. A. Lonneman, F. L. Becker, R. Slater, "Chemical Aspects of the Photo-Oxidation of the Propylene-Nitrogen Oxide System," Environmental Science and Technology, Vol. 1, pp. 899-914, November 1967.

23. S. L. Kopczynski, unpublished data, transmitted October 1969.

24. M. Neiburger, J. Edinger, Meteorology of the Los Angeles Basin With Particular Respect to the "Smog" Problem, Air Pollution Foundation Report No. 1, April 1954.

25. N. Renzetti (ed.), An Aerometric Survey of the Los Angeles Basin August-November 1954, Air Pollution Foundation Report No. 9, July 1955.

REFERENCES (Cont.)

26. L. Fox, Numerical Solution of Ordinary and Partial Differential Equations, Addison-Wesley, Reading, Mass., p. 235, 1962.

27. F. G. Blottner, "Chemical Nonequilibrium Boundary Layer," AIAA Journal, Vol. 2, pp. 232-240, February 1964.

28. J. A. Fay, H. Kaye, "A Finite-Difference Solution of Similar Non-Equilibrium Boundary Layers," AIAA Journal, Vol. 5, pp. 1949-1954, November 1967.

29. F. Pasquill, Atmospheric Diffusion, Van Nostrand & Co., London, p. 72, 1962.

30. C. G. Rossby, R. B. Montgomery, "THE Layer of Frictional Influence in Wind and Ocean Currents," Physical Oceanography and Meteorology, M.I.T. and Woods Hole Oceanographic Institution, Vol. 3, No. 3, 1935.

31. C. H. B. Priestly, Turbulent Transfer in the Lower Atmosphere, University of Chicago Press, pp. 33-38, 1959.

32. A. K. Aleksandrova, N. L. Byzova, G. B. Mashkova, "Experiments on the Spreading of Precipitating Admixture from a Point Source in the Bottom Layer of the Atmosphere," Investigation of the Bottom 300-Meter Layer of the Atmosphere, ed. N. L. Byzova, (tranlated from the Russian by Israel Program for Scientific Translation), Jerusalem, pp. 1-12, 1965.

33. H. Lettau, "A Reexamination of the 'Leipzig Wind Profile' Considering Some Relations Between Wind and Turbulence in the Frictional Layer," Tellus, Vol. 2, pp. 189-200, 1950.

34. V. N. Ivanov, "Statistical Characteristics of Turbulent Diffusion and Their Estimation in the Bottom Layer of the Atmosphere," Investigation of the Bottom 300-Meter Layer of the Atmosphere, ed. N. L. Byzova (translated from the Russian by Israel Program for Scientific Translation), Jerusalem, pp. 36-42, 1965.

35. S. R. Hanna, "A Method for Estimating Vertical Eddy Transport in the Planetary Boundary Layer Using Characteristics of the Vertical Velocity Spectrum," J. of Atmospheric Sciences, Vol. 25, No. 6, pp. 1026-1033, November 1968.

REFERENCES (Cont.)

36. R. A. Craig, "Vertical Eddy Transfer of Heat and Water Vapour in Stable Air," J. of Meteorology, Vol. 6, pp. 122-133, 1949.

37. E. E. Lemke, G. Thomas, W. E. Zwiacher,(eds.), Profile of Air Pollution Control in Los Angeles County, APCD, Los Angeles County, p. 3, January 1969.

38. D. M. Teague, "Los Angeles Traffic Pattern Survey, Vehicle Emissions I," SAE Progress in Technology Series, Vol. 6, pp. 102-120, 1964.

39. Final Report on Phase I, Atmospheric Reaction Studies in the Los Angeles Basin, Vols. I and II, Scott Research Laboratories, June 30, 1969.

40. S. R. Frank, Private communications, July - November 1969.

41. Monthly Reports of Meteorology, Air Pollution Effects and Contaminant Maxima, Air POllution Control District, County of Los Angeles.

42. R. J. Gordon, H. Mayrsohn, R. M. Ingels, "C_2-C_5 Hydrocarbons in the Los Angeles Atmosphere," Environmental Science and Technology, Vol. 2, pp. 1117-1120, December 1968.

43. A. P. Altshuller, S. L. Kopczynski, D. Wilson, W. Lonneman, F. D. Sutterfield, "Photochemical Reactivities of Parrafinic Hydrocarbon Nitrogen Oxide Mixtures Upon Addition of Propylene or Tolyene," J. Air Poll. Control Assoc., Vol. 19, pp. 791-794, 1969.